



(51) International Patent Classification:

A61F 5/00 (2006.01) A61F 9/007 (2006.01)  
A61F 9/00 (2006.01) A61F 9/008 (2006.01)

(21) International Application Number:

PCT/US2019/029636

(22) International Filing Date:

29 April 2019 (29.04.2019)

(25) Filing Language:

English

(26) Publication Language:

English

(30) Priority Data:

16/203,970 29 November 2018 (29.11.2018) US

(71) Applicant: **OJAI RETINAL TECHNOLOGY, LLC**  
[US/US]; 283 Carne Road, Ojai, California 93023 (US).

(72) Inventors: **LUTTRULL, Jeffrey K.**; 283 Carne Road, Ojai, California 93023 (US). **CHANG, David B.**; 14212 Livingston, Tustin, California 92780 (US).

(74) Agent: **KELLEY, Scott W.**; Kelly & Kelley, LLP, 6320 Canoga Avenue, Suite 1650, Woodland Hills, California 91367 (US).

(81) Designated States (unless otherwise indicated, for every kind of national protection available): AE, AG, AL, AM, AO, AT, AU, AZ, BA, BB, BG, BH, BN, BR, BW, BY, BZ, CA, CH, CL, CN, CO, CR, CU, CZ, DE, DJ, DK, DM, DO, DZ, EC, EE, EG, ES, FI, GB, GD, GE, GH, GM, GT, HN, HR, HU, ID, IL, IN, IR, IS, JO, JP, KE, KG, KH, KN, KP, KR, KW, KZ, LA, LC, LK, LR, LS, LU, LY, MA, MD, ME, MG, MK, MN, MW, MX, MY, MZ, NA, NG, NI, NO, NZ, OM, PA, PE, PG, PH, PL, PT, QA, RO, RS, RU, RW, SA, SC, SD, SE, SG, SK, SL, SM, ST, SV, SY, TH, TJ, TM, TN, TR, TT, TZ, UA, UG, US, UZ, VC, VN, ZA, ZM, ZW.

(84) Designated States (unless otherwise indicated, for every kind of regional protection available): ARIPO (BW, GH, GM, KE, LR, LS, MW, MZ, NA, RW, SD, SL, ST, SZ, TZ, UG, ZM, ZW), Eurasian (AM, AZ, BY, KG, KZ, RU, TJ, TM), European (AL, AT, BE, BG, CH, CY, CZ, DE, DK,

(54) Title: PROCESS FOR ADJUSTING TREATMENT PARAMETERS FOR RETINA PHOTOTHERAPY BASED ON RPE MELANIN LEVELS

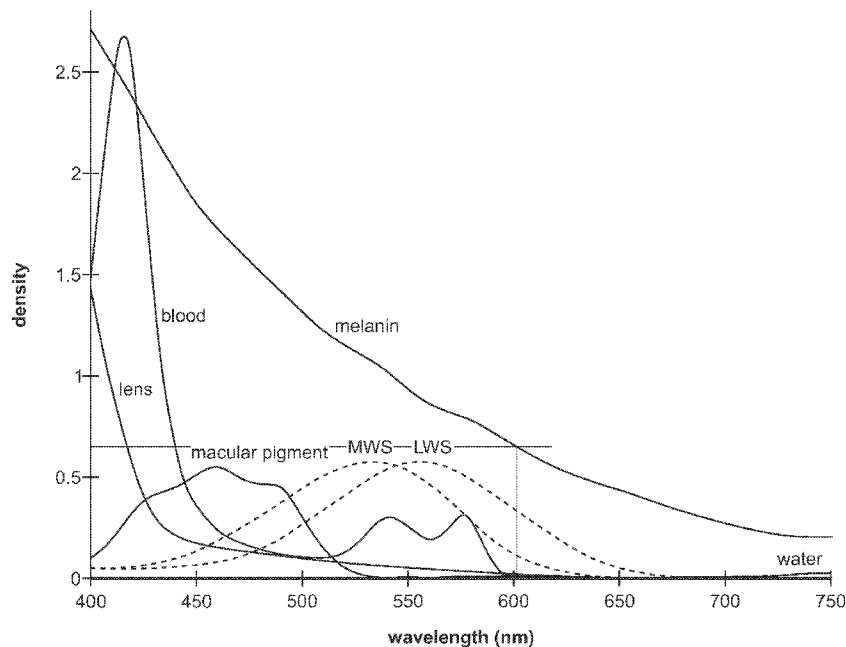


FIG. 3

(57) Abstract: A process for safely providing retinal phototherapy includes generating first and second light beams of a different wavelength. The first and second light beams are applied to a retinal pigment epithelium (RPE) and choroid of an eye. The amount of light reflected from the eye from the first light beam and the second light beam is measured, such as using a reflectometer. A level or concentration of the melanin within the eye is calculated using the measured amount of light reflected from the eye from the first and second light beams. When the content or density of melanin in the RPE exceeds a predetermined amount, one or more treatment parameters of the retinal phototherapy is adjusted.



EE, ES, FI, FR, GB, GR, HR, HU, IE, IS, IT, LT, LU, LV,  
MC, MK, MT, NL, NO, PL, PT, RO, RS, SE, SI, SK, SM,  
TR), OAPI (BF, BJ, CF, CG, CI, CM, GA, GN, GQ, GW,  
KM, ML, MR, NE, SN, TD, TG).

**Published:**

— *with international search report (Art. 21(3))*

**PROCESS FOR ADJUSTING TREATMENT PARAMETERS FOR RETINA  
PHOTOTHERAPY BASED ON RPE MELANIN LEVELS**

**DESCRIPTION**

**FIELD OF THE INVENTION**

[Para 1] The present invention generally relates to a process for safely providing retinal phototherapy. More particularly, the present invention is directed to a process for safely providing retinal phototherapy by adjusting treatment parameters of the retinal phototherapy based on retinal pigment epithelium (RPE) melanin levels determined, such as using a simple reflectometry process.

**BACKGROUND OF THE INVENTION**

[Para 2] The importance of macular pigment to the health of the eye has prompted development and interest in methods for measuring its density or concentration in the retina. Prior systems and methods, however, have either been based upon equipment which is not commonly available, is time consuming, or complicated and expensive.

[Para 3] With reference now to FIG. 1, a diagrammatic view of an eye, generally referred to by the reference number 10, is shown. The eye 10 includes a cornea 12 which is a transparent front part of the eye that covers the iris and pupil 14 which is the variable-size black circular or slit-shaped opening in the

center of the iris that regulates the amount of light that enters the eye. The lens 16 is a transparent biconvex structure in the eye that, along with the cornea 12, helps to refract light to be focused on the retina 18. The retina is a thin layer of neural cells that line the back of the eyeball which captures light and transforms it into electrical signals for the brain. It has many blood vessels 20 to nourish it. The fovea and macular region, referred to by the reference number 22, is a portion of the eye used for color vision and fine detail vision. The retinal pigmented epithelium (RPE) 24 is the pigmented cell layer just outside the neurosensory retina 18 that nourishes the retinal visual cells. It is firmly attached to an underlying choroid 26 which is a vascular layer of the eye 10 lined between the retina 18 and the sclera. The choroid 26 provides oxygen and nourishment to the outer layers of the retina 18.

[Para 4] Many diseases of the eye are related to the retina and there have been developed methodologies including photocoagulation and photostimulation of the retina to treat such diseases and conditions. Photocoagulation and photostimulation rely upon heating of the retinal tissue to create their therapeutic effects. Excessive heating can damage or even destroy retinal tissue, which in some treatment methodologies is intentional but in others is avoided. It has been found that abnormal levels of pigmentation, particularly levels or concentrations of melanin within the RPE, can cause unanticipated and excessive heat during such treatments and potentially damage the retinal tissue.

[Para 5] Melanin in the eye has many important functions which are not yet completely understood. Melanin in the eye provides protection to the eye by absorbing harmful ultraviolet radiation. Melanin promotes visual acuity by scattering stray light away from the rods and cones and absorbing light reflected from the back of the eye. Melanin also serves as an antioxidant to aid in the prevention of retinal diseases, such as age-related macular degeneration.

[Para 6] Many of these properties result from the fact that the absorption spectrum of melanin is very broad. In this respect, it is unique among pigments. Many mechanisms have been suggested for this unique behavior. As examples, the broadband absorption has been attributed to chemical heterogeneity, amorphous semiconducting, and scattering. However, it has been shown that scattering losses only account for a few percent of the broadband attenuation. There are also problems with the chemical heterogeneity and amorphous semiconducting hypothesis. Some have proposed polymeric charge hopping. Others have pointed out the importance of hydration and introducing free radicals into melanin. Yet others have suggested that melanin excitons may play a role in its broadband absorption. There does not appear to be universal agreement that any particular explanation can account for all of melanin's electrical and optical properties.

[Para 7] As indicated above, melanin within the eye serves many important functions. The determination of the levels or concentrations of melanin within the eye can be important to ascertain. For example, laser treatments of eye diseases are based on inducing temperature rises in the RPE, which activates

the eye's natural repair mechanisms. In the near infrared, this results from the absorption of the infrared radiation by the melanin pigment in the RPE.

Considerable melanin also exists in the choroid behind the RPE, but absorption by the choroidal melanin does not play a significant role in raising the temperature of the RPE due to the lack of diffusive heat transfer to the RPE during the relatively short treatment times and due to the convective cooling by the blood vessels in the choroid and the choriocapillaris.

[Para 8] In laser subthreshold damage treatments of eye diseases, the laser treatment is effective as long as the temperature rise does not exceed the order of 10° C. This temperature rise limitation determines the maximum laser energy that can be absorbed by the RPE during the treatment time. A possible concern, however, is that for laser powers that are suitable for most patients, the temperature rise can exceed the threshold for damage if the patient's RPE melanin content or concentration is abnormally too large.

[Para 9] Accordingly, there is a continuing need for a simple and relatively inexpensive process for determining melanin levels or concentrations within the eye, and particularly within the RPE of the eye, so that one or more treatment parameters of the retinal phototherapy treatment can be adjusted as needed to avoid damaging patient's eyes who have an abnormally large content or concentration of melanin in the RPE. The present invention fulfills these needs, and provides other related advantages.

## SUMMARY OF THE INVENTION

[Para 10] The present invention is directed to a process for safely providing retinal phototherapy by adjusting one or more treatment parameters of the retinal phototherapy if the content or concentration of melanin in the RPE of the eye exceeds a predetermined amount. The present invention uses a two-wavelength reflectometry process for determining the levels or concentrations of melanin in the RPE and choroid of the eye, which is relatively simple and inexpensive.

[Para 11] In accordance with the present invention, a first light beam having a wavelength between 550 nm and 900 nm is generated. The first light beam may have a wavelength of between 600 nm and 850 nm. The first light beam is applied into the eye, such as being applied to a retinal pigment epithelium (RPE) and a choroid of the eye. The amount of light reflected from the eye from the first light beam is measured. This may be done by using a reflectometer to measure the amount of light reflected from the eye from the first light beam.

[Para 12] A second light beam having a wavelength between 550 nm and 900 nm is generated. The second light beam may have a wavelength between 600 nm and 850 nm. The second light beam is of a different wavelength than the first light beam. The first and second light beams preferably differ in wavelength by at least 25 nm. The second light beam is applied into the eye, such as to the RPE and choroid of the eye. The amount of light reflected from the eye from the second light beam is measured, such as using a reflectometer.

[Para 13] The level of melanin within the eye is calculated using the measured amount of light reflected from the eye from the first and second light

beams. More particularly, the calculating step includes the step of distinguishing the amount of light reflected by the first and second light beams from the RPE and the choroid.

[Para 14] One or more treatment parameters of the retinal phototherapy is adjusted if the content or concentration of melanin in the RPE of the eye exceeds a predetermined amount. This can comprise adjusting at least one of a retinal spot size of a treatment light beam, a pulse train duration of the treatment light beam, a duty cycle of the treatment light beam, or a power of the treatment light beam. For example, a retinal spot size of the treatment light beam may be increased. A pulse train duration of the treatment light beam may be lowered. A duty cycle of the treatment light beam may be lowered. A power of the treatment light beam may be lowered.

[Para 15] The one or more treatment parameters are adjusted when the content of melanin in the RPE of the eye is determined to be at least four times greater than a normal content of melanin in the RPE. For example, if the content of the melanin in the RPE is determined to be four to eight times a normal melanin content of the RPE, for pulse train durations of the pulsed light beam retina therapy ranging from 0.2 to 0.5 seconds, one or more treatment parameters are adjusted. For example, the one or more treatment parameters are adjusted when the content of the melanin in the RPE is determined to be greater than  $8 \times 10^{10} \text{cm}^{-3}$ .

[Para 16] The one or more treatment parameters of the retina therapy system may be automatically adjusted when the content of the melanin in the RPE of

the eye exceeds the predetermined amount. A notification may be given that one or more retinal treatment parameters have been adjusted.

[Para 17] Other features and advantages of the present invention will become apparent from the following more detailed description, taken in conjunction with the accompanying drawings, which illustrate, by way of example, the principles of the invention.

#### BRIEF DESCRIPTION OF THE DRAWINGS

[Para 18] The accompanying drawings illustrate the invention. In such drawings:

[Para 19] FIGURE 1 is a diagrammatic view of an eye;

[Para 20] FIGURE 2 is a diagrammatic view of a system used in accordance with the present invention for determining concentrations of melanin within portions of an eye;

[Para 21] FIGURE 3 is a graph illustrating wavelength dependence of the absorption of primary ocular pigments;

[Para 22] FIGURE 4 is a graph illustrating absorbance of eumelanin as a function of wavelength;

[Para 23] FIGURE 5 is a graph depicting two-way transmission through RPE melanin at ordinary concentrations;

[Para 24] FIGURE 6 is a graph illustrating variation of the RPE melanin transmission at different wavelengths;

[Para 25] FIGURE 7 is a graph illustrating angular distribution of an intensity function that is proportional to the differential cross-section for scattering from a prolate spheroid and spheres;

[Para 26] FIGURE 8 is a graph depicting a comparison of RPE melanin absorption coefficient, melanin scattering coefficient, and structural matrix scattering coefficient;

[Para 27] FIGURE 9 is a graph depicting a comparison of choroid melanin absorption coefficient, choroid melanin scattering coefficient, and choroid structural matrix scattering coefficient;

[Para 28] FIGURE 10 is a graph depicting the reflectivity of choroid as a function of wavelength at a normal choroid melanosome density;

[Para 29] FIGURE 11 is a graph depicting the reflectivity of RPE as a function of wavelength at normal RPE and choroid melanosome densities;

[Para 30] FIGURE 12 is a graph depicting a transmission factor of anterior retina versus wavelength;

[Para 31] FIGURE 13 is a graph depicting percentage changes in total reflectivity as a function of wavelength as RPE and choroid melanosome densities vary from the normal;

[Para 32] FIGURE 14 is a contour plot at a first wavelength of percentage change in the total reflectivity in accordance with two-wavelength reflectometry, in accordance with the present invention;

[Para 33] FIGURE 15 is a contour plot at a second wavelength of the percentage change in the total reflectivity in accordance with two-wavelength reflectometry, in accordance with the present invention;

[Para 34] FIGURE 16 is a graph showing the damage ratio of abnormal RPE melanin content to normal RPE melanin content at which damage can occur compared to a pulse train duration of pulsed light phototherapy; and

[Para 35] FIGURE 17 is a graph similar to FIG. 16, illustrating the damage ratio in a range of 200 milliseconds to 500 milliseconds of light phototherapy pulse train duration.

#### DETAILED DESCRIPTION OF THE PREFERRED EMBODIMENTS

[Para 36] For purposes of illustration, the present invention is directed to a process for safely providing retinal phototherapy by determining concentrations of melanin within an eye, and particularly within the retinal pigment epithelium (RPE) and choroid of the eye. Determining the concentrations or levels of melanin within the RPE and choroid of the eye can be important in determining the health of the eye. For example, melanin functions as an antioxidant to aid in the prevention of retinal diseases, such as age-related macular degeneration. Determining the concentrations of melanin within the RPE or choroid of the eye can also be important in determining treatment of eye diseases. For example, if an individual has abnormally elevated concentrations or levels of melanin within the RPE this can cause unanticipated elevated heating, and thus tissue destruction, when treating the eye, and particularly the retina, with light

sources, such as infrared or near infrared laser light beams, such as those used in retinal phototherapy, such as photocoagulation or photostimulation.

[Para 37] The melanin layers within the choroid can vary significantly. However, it is the level or concentrations of melanin within the RPE that is often important to determine as this is the layer which can cause excessive heating and damage when the retina is exposed to light sources during photocoagulation or photostimulation treatments. The invention takes into account the light absorbed and scattered by both the RPE and choroid layers in order to get an accurate picture of the amount of melanin in the RPE. The invention, as will be more fully described herein, utilizes two wavelengths within a predetermined range of wavelengths in which melanin both absorbs and reflects these wavelengths. The wavelengths are distinct from one another, preferably towards the lower end and the upper end of the predetermined wavelength range, and the present invention measures the amount or degree of reflections and then determines the levels or concentrations of melanin within the RPE and choroid by taking into account both the absorption and the scattering or reflections of the two wavelengths.

[Para 38] With reference now to FIG. 2, a system 100 is shown which is used in accordance with the present invention. Laser console 102 generates a first light beam having a wavelength within a predetermined range. The range may be between 550 nm and 900 nm, typically between 600 nm and 850 nm. Wavelengths below the predetermined wavelength range begin to absorb and scatter light from other pigments, and wavelengths above the predetermined

range of wavelengths of the present invention are increasingly absorbed by water. However, the predetermined wavelength range of the present invention is ideal for measuring the melanin levels of the RPE and choroid.

[Para 39] The generated light beam is then passed through optics 106, which may be used to focus the light beam, filter the light beam, generate a plurality of light beams from the generated first light beam, or the like. The light beam is then passed through projector 108, which may be a retina camera or the like, for projection into the eye 10, and more particularly so as to apply the first light beam to the RPE 24 and choroid 26 of the eye 10. Reflections from the RPE and choroid are detected by detector 110. The detector 110 in a particularly preferred embodiment is a reflectometer although other detector devices could be utilized such as those using interferometry such as an Optical Coherent Tomography (OCT) device.

[Para 40] With continuing reference to FIG. 2, a second light beam is generated, such as by laser console 104. The second light beam has a wavelength between 550 nm and 900 nm, preferably 600 nm–850 nm, that is a different wavelength than the first light beam. The first and second light beams preferably differ in wavelength by at least 25 nm, and more preferably are near opposite ends or ranges of the wavelength range so that they can be more easily distinguished from each other when the light reflected by each is detected.

[Para 41] The second light beam may pass through optics 106, as described above, and then through projector 108 into the eye 10, and particularly the RPE

and choroid 24 and 26 of the eye 10. The light scattered and reflected by the second light beam is detected and measured by detector 110. It will be understood that the first and second light beams generated by consoles 102 and 104 can be applied to the eye 10 sequentially or simultaneously.

[Para 42] The amount of light reflected from the RPE and the choroid by the first and second light beams is measured, and then a concentration of melanin within the RPE and choroid of the eye is determined using the measured amount of light reflected from the RPE and the choroid from the first and second light beams. The invention distinguishes the amount of light reflected by the first and second light beams from the RPE and the choroid and the measurements of the amount of light reflected from the first and second light beams may be applied to calculations and/or graphs or tables to determine the levels or concentrations of melanin within the choroid and more particularly the RPE. The determined level or concentration of melanin within the RPE can then be compared to anticipated or average levels of melanin within the RPE to determine if the melanin levels within the RPE of that eye are elevated or outside of the anticipated range.

[Para 43] The melanin in the eye is primarily eumelanin, and its monomer has the chemical formula  $C_{18}H_{10}N_2O_4$ , and a molecular weight of 318.283, with a density of 1.7 g/cc and an index of refraction of 1.772. In both the RPE and the choroid, melanin is contained in protein-coded organelles, called melanosomes. Inside the melanosomes, the melanin monomers, which have dimensions of less than ten Angstroms, combine to form aggregates. The

aggregates have dimensions of several tens of Angstroms, and are made up of stacked sheets of covalently-bonded monomer, with the sheets having separations of 3.4 Angstroms. The sheets are held together by weaker pi-pi bonding forces.

[Para 44] The melanin in the RPE is derived from the neural ectoderm, whereas the choroidal melanin is derived from the neural crest. The melanosomes in the RPE are different from those in the choroid. In the RPE, the melanosomes are located mainly in the apical region of the RPE cells and are elongated in shape, with the long dimension aligned with the apices in order to make close contact with the rods and cones. Typical widths of all foreign RPE melanosome are 250–500 nm, and typical lengths are 640–800 nm. These give  $6.5 \times 10^{-14}$  cubic centimeters for a typical melanosome volume. The melanin is rather densely packed in the RPE melanosomes, the melanin density in a monomer being 1.7 g/cc.

[Para 45] In the choroid, the melanosomes do not need to be elongated and are believed to be globular in shape. The density of melanin in the choroid is less than that in the RPE, with ranges of 3.61–8.05 mmol/L for RPE melanin, and 0.07–9.15 mmol/L for choroidal melanin. However, since the choroid depth is 200 microns compared to 6–10 microns for the REP, there is much more melanin in the choroid than in the RPE.

[Para 46] In the RPE, from the foregoing numbers, the number density of melanin is  $3.38 \times 10^{18}$  cm<sup>-3</sup> with a mass density of  $1.8 \times 10^{-3}$  g/cc, and since the melanin is all contained within melanosomes, the corresponding number

density of melanosomes in the RPE is  $10 \times 10^{10} \text{ cm}^{-3}$ . This gives a linear separation between melanosomes in the RPE of 3.68 microns. In the choroid, on the other hand, the density of melanin is  $0.49 \times 10^{-3} \text{ g/cc}$ , corresponding to a melanosome number density of  $5.4 \times 10^9 \text{ cm}^{-3}$ . Thus, in the choroid, the linear spacing between the melanosomes is  $5.7 \times 10^{-4} \text{ cm}$ , or 5.7 microns.

[Para 47] With reference now to FIG. 3, the absorption of blood, melanin, macular pigments, the lens, water, long wavelength sensitive visual pigments (LWS) and medium wavelength sensitive visual pigments (MWS) primarily within the visible range of wavelengths is illustrated. The blood layer is taken to be 23 microns thick with an oxygenation of 95%. The melanin density is 1.32 at 500 nm, and the macular density is 0.54 at 460 nm. The lens density is 0.54 at 420 nm and the water density is 0.025 at 740 nm. The visual pigment densities are both 0.57 at their peaks. In the eye, melanin dominates the absorption of laser light in the wavelength range generally between 550 nm and 900 nm, and more particularly between 600 nm and 850 nm as shown in FIG. 3.

[Para 48] Prior modeling of the spectral reflectance of the human eye used values of 3.61–8.05 mmol/L for RPE melanin and values of 0.07–9.15 mmol/L for choroidal melanin. The thickness of the melanin layer in the RPE is less than 10 microns, typically around 6 microns, whereas the choroid thickness is on the order of 200 microns, or approximately 30 times thicker. Thus, much more melanin usually exists in the choroid than in the RPE. Moreover, it has been found that the melanin content in the RPE does not usually vary much from patient to patient, although the choroid melanin can vary widely.

[Para 49] As seen in FIG. 3, the absorption coefficient of melanin decreases considerably as the wavelength increases. Thus, at the lower 600 nm end of the melanin-dominated absorption window, the RPE melanin absorption is much larger than it is at the 850 nm upper end of a particularly preferred range of wavelengths. There is no general agreement as to how the melanin absorption varies with wavelength, however.

[Para 50] FIGURE 4 is a graph illustrating the absorbance of eumelanin as a function of wavelength, particularly between 250 nm and 700 nm. Eumelanin is the dominant component of the melanin in the eye. Although there is no general agreement on the variation of the optical density with wavelength, the present invention assumes exponential dependence of  $\exp[-0.062\lambda(\text{nm})]$ , which is reflected in FIG. 4. If this result is combined with the prior finding of an optical density of 0.22 at 500 nm, this gives for the two-way transmission through the RPE of:

[Para 51]  $\text{Transmission} = \exp[-2\alpha L] = \exp[-22.72 \exp[-0.0062 \lambda(\text{nm})]]$  [1]

[Para 52] On the other hand, if an optical density of 0.29 at 500 nm is used, then the result yields:

[Para 53]  $\text{Transmission} = \exp[-2\alpha L] = \exp[-29.973 \exp[-0.0062 \lambda(\text{nm})]]$  [2]

[Para 54] Equations [1] and [2] are plotted in FIG. 5, which is a graph depicting the two-way transmission (as determined by the large absorption cross-section) through the RPE melanin at ordinary concentrations. The top curve assumes that the optical density is 0.22 at 500 nm, whereas the lower curve assumes that the optical density at 500 nm is 0.29. It can be seen that

towards the 850 nm limit of the melanin-dominated absorption window, the absorption coefficient of the RPE melanin is small, permitting the reflected signal from the choroid to pass through to the detector 110. However, at the 600 nm lower limit, the absorption coefficient of RPE melanin becomes sufficiently large that less of the reflected signal from the choroid can pass through to the detector. At elevated, potentially dangerous, levels of RPE melanin, the reflected signal from the choroid at 600 nm is diminished considerably on passing through the RPE, while at 800 nm is not diminished nearly as much.

[Para 55] FIGURE 6 is a graph illustrating the variation of the RPE melanin transmission (as determined by the large absorption coefficient) at 750 nm (top curve) and at 600 nm (bottom curve) as the RPE melanin concentration is varied from normal ( $n=1$ ) to an elevated, danger threshold of three times normal ( $n=3$ ). In FIG. 6, it is assumed that the optical density of 500 nm is 0.22 for a normal RPE concentration. With continuing reference to FIG. 6, the graph shows the behavior of the RPE melanin transmission at 600 nm and 750 nm as the concentration is varied from normal ( $n=1$ ) to a dangerous level of three times normal ( $n=3$ ). The graph of FIG. 6 shows that at 600 nm the transmitted signal is diminished by a factor of close to 4, while at 750 nm it is only diminished by a factor of approximately 1.5. This large difference, however, may be mitigated somewhat by other factors in the expression for reflectivity.

[Para 56] By contrast, the optical path in the melanin in the choroid is larger. It has been estimated that the typical density of melanin in the RPE is 5.82

mmol/L, and since the molecular weight of melanin monomer is 318.283, a weight density of  $1.86 \times 10^{-3} \text{g/cc}$  is given. This occupies a region of thickness of 6–10 microns. For the choroid, a typical density of 1.59 mmol/L, i.e.  $0.51 \times 10^{-3} \text{g/cc}$ , but the thickness of the choroid is 200 microns. Thus, if the optical density of the RPE melanin is 0.22 at 500 nm, the choroid melanin has an optical density at 500 nm of 2.00. Thus, one-way transmission from the back to the front of the choroid is only  $\exp[-2.303 \times 2.00] = 0.01$ . Thus, most of the radiation is absorbed. This means that the reflection from the sclera does not contribute appreciably to the reflection signal. However, there is considerable variation in the choroid melanin content in different eyes and patients, so it is important in general to take account of the contribution of a reflection from the sclera.

[Para 57] Melanin is densely packed in the melanosomes. As described above, in the RPE the melanosomes are elongated in shape and make close contact with the rods and cones. In the choroid, on the other hand, the melanosomes are believed to be globular in shape. The melanosomes are regarded as the basic scattering entities. The melanosomes have dimensions comparable to the 600 nm–850 nm wavelengths of interest. A typical RPE melanosome has dimensions of 250–400 nm (average 300 nm) wide by 640 nm–800 nm (average 720 nm) long. It is assumed that a globular choroid melanosome has a comparable volume to an RPE melanosome, so as to have a radius of  $2.5 \times 10^{-5} \text{cm}$ , i.e. 250 nm.

[Para 58] For dielectric spherical scatterers, when the radiation wavelength is much larger than the size of the scatter, the cross-section for the scattering may be given by the Rayleigh expression:

$$[\text{Para 59}] \quad \sigma_{\text{Rayleigh}} = (8\pi/3)(ka)^4 a^2 \{(K_{\text{rel}} - 1)/(K_{\text{rel}} + 2)\}^2 \quad [3a]$$

[Para 60] Whereas when the wavelength is comparable to the size of the scatterer, the cross section is expressed in terms of the Mie sum over an infinite series of Legendre polynomials. At small wavelengths, the Mie expression for the total scattering cross section reduces to the asymptotic value:

$$[\text{Para 61}] \quad \sigma_{\text{sphere}} = 2\pi a^2 \quad [3b]$$

[Para 62] In eqs. [3a] and [3b], the wave number  $k$  is:

$$[\text{Para 63}] \quad k = 2\pi n_{\text{med}}/\lambda \quad [3c]$$

and

- $a$  = radius of scattering sphere
- $n_{\text{med}}$  = index of refraction of the medium in which the sphere is immersed
- $\lambda$  = vacuum wavelength of the radiation
- $K_{\text{rel}} = n_{\text{sphere}}/n_{\text{med}}$
- $n_{\text{sphere}}$  = index of refraction of the sphere

[Para 64] When  $ka = O(1)$ , the cross section oscillates a little as it approaches its asymptotic value of  $\sigma_{\text{sphere}} = 2\pi a^2$ .

[Para 65] Another important difference in the behavior of the scattering at long and short wavelengths is that at long wavelengths, there are approximately as many scattering events in the forward as in the backward

direction. At short wavelengths, however, this changes dramatically when  $ka > 1$ , the scattering is predominantly in the forward direction. The scattering angles are contained mainly in a cone of angle:

$$\text{[Para 66]} \quad \vartheta = O(1/ka) \quad [4]$$

[Para 67] Thus, on applying the Born approximation to a spherical scatterer of radius  $a$ , it can be shown that:

$$\text{[Para 68]} \quad \langle \cos\vartheta \rangle = g[2kasin\vartheta] \quad [5a]$$

where

$$\text{[Para 69]} \quad g(x) = (\sin x - x \cos x)^2 / x^6 \quad [5b]$$

[Para 70] When  $ka \gg 1$ , this reduces to:

$$\text{[Para 71]} \quad \langle \cos\vartheta \rangle = 1 - (5/4)(1/(ka))^2 \quad [5c]$$

[Para 72] showing that at short wavelengths, the scattering angle is very small.

[Para 73] The cross section  $\sigma_s$  for a sphere to scatter in backward directions when  $ka \gg 1$  is then:

$$\text{[Para 74]} \quad \sigma_{s \text{ SPHERE}} = 2\pi a^2 [1 - \langle \cos\vartheta \rangle] = 2\pi a^2 (5/4)(1/(ka))^2 = (5/8\pi)\lambda^2 = 0.08 \lambda^2 \quad [5d]$$

[Para 75] in the Born approximation, independent of its radius, and just proportional to the square of the wavelength. Since eq. [5d] is derived using the Born approximation, the 0.08 coefficient may not be correct, but the dependence on  $\lambda^2$  is believable since it results from diffraction on a sphere of radius  $a$ .

[Para 76] The melanosomes in the RPE are not spherical in shape, but are elongated with their long dimensions oriented parallel to the axes of the rods and cones. The melanosomes are comprised of melanin aggregates made up of stacked sheets of covalently bonded melanin monomers.

[Para 77] With reference to FIG. 7, a graph provides the information needed to estimate the scattering cross-section of a prolate spheroid that has the dimensions of an RPE melanosome. FIG. 7 shows angular distribution of an intensity function that is proportional to the differential cross-section for scattering from a prolate spheroid with  $a/b=2$  and  $kc=5$  (dashed line), and from three spheres for comparison (solid lines). The solid line curve labeled "2" is for a sphere of the same volume as a prolate spheroid. The figure shows the resemblance of the scattering behavior to that described by Mie scattering from spheres.

[Para 78] In FIG. 7, the semi major axis of the prolate spheroid is denoted by "a" and corresponds to one-half of the 720 nm (640–800 nm) dimension of the RPE melanosome. The semi minor axis of the prolate spheroid is denoted by "b", and corresponds to one-half of the 300 nm (250–400 nm) dimension of the RPE melanosome. The wave number defined in equation [3c] is "k". The semifocal distance is  $c=(a^2-b^2)^{1/2}$ . The radiation is assumed to be incident on the prolate spheroid along its major axis. The aspect ratio ( $a/b=2$ ) of the prolate spheroid in FIG. 7 is comparable to that of an RPE melanosome ( $a/b=2.4$  on average).

[Para 79] The differential cross section for scattering is proportional to the intensity function of the ordinate in the figure. Accordingly, measurement of the areas under the dashed curve and under the solid curve of the sphere of equal volume (labeled “2”) in the figure reveals that the cross section for forward scattering (0 to 90 degrees) in the prolate spheroid is 1.45 times that for forward scattering from a sphere of equal volume. Also, the cross section for backwards scattering (90–180 degrees) in the prolate spheroid is 0.6 that for backwards scattering from a sphere of equal volume. That means that a choroidal melanosome is 1.65 times more effective than an RPE melanosome in scattering radiation in the backwards direction. For the sphere, the ratio of the backwards scattering cross section to the total scattering cross section is 0.018, i.e. only 1.8% of the scattered radiation is in the backwards direction. This is consistent with our earlier observation that most of the radiation is scattered in a small cone about the forward direction (eq. [4]).

[Para 80] Taking the total scattering cross section of the sphere to be  $2\pi a^2$  (eq. [3b]), the last observation allows us to say that the sphere’s cross section for backwards scattering is:

$$\begin{aligned} \text{[Para 81]} \quad \sigma_s(\text{sphere}) &= 0.018 \times 2\pi a^2 = 0.018 \times 2\pi \times (2.5 \times 10^{-5})^2 = \\ &0.707 \times 10^{-10} \text{ cm}^2 \end{aligned} \quad [6]$$

at a wavelength corresponding to  $kc = 5$ .

[Para 82] To determine the wavelength for which eq. [6] applies, examine the expression for  $kc=5$ :

$$\text{[Para 83]} \quad Kc = ka[1-(b/a)^2]^{1/2} = 5 \quad [7a]$$

i.e.

[Para 84]  $(2\pi/\lambda)360[1-0.25]^{1/2} = 5$  [7b]

[Para 85] This gives  $\lambda = 39$  nm. Accordingly, since eq. [5d] indicates that the backwards scattering cross section should be proportional to  $\lambda^2$ , we find for a general wavelength less than  $2\pi a = 1571$  nm,

[Para 86]  $\sigma_{sCH} \approx 0.43 \times 10^{-10} (\lambda_{nm}/392)^2 = 0.05 \lambda^2 \text{ cm}^2$  [8a]

[Para 87] This is a little smaller than the  $0.08 \lambda^2 \text{ cm}^2$  Born approximation result of eq. [5d]. From the measured 0.6 ratio of the backwards scattering cross sections of prolate spheroids and spheres of the same volume in FIG. 7, and the expected diffraction-related origin of the  $\lambda^2$  dependence, we then write for the backwards scattering cross section of an RPE melanosome:

[Para 88]  $\sigma_{sRPE} \approx 0.03 \lambda^2 \text{ cm}^2$  [8b]

[Para 89] When  $\lambda$  is expressed in terms of nm, eqs. [8] and [9] become:

[Para 90]  $\sigma_{sCH} \approx 0.03 \times 10^{-14} \lambda_{nm}^2 \text{ cm}^2$  [9a]

[Para 91]  $\sigma_{sRPE} \approx \approx 0.05 \times 10^{-14} \lambda_{nm}^2 \text{ cm}^2$  [9b]

[Para 92] Although the absorption is dominated by the melanin in the 600 nm–800 nm range of wavelengths, scattering can also result from the structural matrix in which the melanosomes are embedded. Prior research has determined the scattering properties of the retina and the choroid from OCT scans. For a wavelength of 855 nm:

[Para 93] Retina:

- Scattering coefficient  $1.64 \times 10^{-4} \lambda_{nm}^2 t_{RET} = 120 \text{ cm}^{-1}$
- Anisotropic factor  $g_{RET} = \langle \cos\theta \rangle = 0.97$

[Para 94] Choroid:

- Scattering coefficient  $\mu_{\text{scatCH}} = 275 \text{ cm}^{-1}$
- Anisotropic factor  $g_{\text{CH}} = 0.90$

[Para 95] With the large anisotropic factor, the backwards scattering coefficient is obtained from the scattering coefficient by multiplying it by  $(1-g)$ .

[Para 96] The scattering occurs due to mismatches in refractive index of the different tissue components, ranging from cell membranes to whole cells. Cell nuclei and mitochondria are the most important scatterers. Their dimensions range from 100 nm to 6  $\mu\text{m}$ , and thus fall within the NIR window. Most of these organelles fall in the Mie region, and exhibit highly anisotropic forward-directed scattering.

[Para 97] As the above only gives a scattering coefficient anisotropic factor for the entire retina, and not for the RPE layer that forms the back layer of the retina individually, the RPE scattering coefficient and an anisotropic factor is approximated by using the total retinal quantities. As the scattering coefficient is only given at a single wavelength and since the scattering has been determined as being primarily in the Mie region,

[Para 98] We shall apply the  $\lambda^2$  factor of eq.[5.9] to determine the scattering coefficients at other wavelengths:

- $\mu_{\text{backscatRET}} = (1-0.97) 120 (\lambda_{\text{nm}} / 855)^2 = 4.92 \times 10^{-6} \lambda_{\text{nm}}^2 \text{ cm}^{-1}$  [10a]
- $\mu_{\text{backscatCH}} = (1-0.90) 275 (\lambda_{\text{nm}} / 855)^2 = 3.76 \times 10^{-5} \lambda_{\text{nm}}^2 \text{ cm}^{-1}$  [10b]

[Para 99] These can be compared with the scattering coefficients from melanin for normal melanosome densities ( $N_{\text{RPE}} = 2 \times 10^{10} \text{ cm}^{-3}$  and  $N_{\text{CH}} = 5.4 \times 10^9 \text{ cm}^{-3}$ )

- $\mu_{\text{sRPE}} = 2 \times 10^{10} \times 0.05 \times 10^{-14} \lambda_{\text{nm}}^2 = 1 \times 10^{-5} \lambda_{\text{nm}}^2 \text{ cm}^{-1}$  [normal RPE melanin density] [11a]

- $\mu_{\text{sCH}} = 5.4 \times 10^9 \times 0.03 \times 10^{-14} \lambda_{\text{nm}}^2 = 1.62 \times 10^{-6} \lambda_{\text{nm}}^2 \text{ cm}^{-1}$  [normal choroid melanin density] [11b]

[Para 100] We see that scattering from the structural matrix in the RPE is less than that from the melanin, whereas in the choroid the scattering from the structural matrix is larger by an order of magnitude.

[Para 101] The scattering coefficients are smaller than the coefficients of absorption at normal melanin densities

- $\mu_{\text{aRPE}} = 2 \times 10^{10} \times 9.47 \times 10^{-7} \exp[-0.0062 \lambda_{\text{nm}}] = 1.89 \times 10^4 \exp[-0.0062 \lambda_{\text{nm}}]$  [12a]

- $\mu_{\text{aCH}} = 5.4 \times 10^9 \times 9.47 \times 10^{-7} \exp[-0.0062 \lambda_{\text{nm}}] = 5.11 \times 10^3 \exp[-0.0062 \lambda_{\text{nm}}]$  [12a]

[Para 102] The melanosome number densities and scattering cross sections indicate that not much scattering occurs in traversing either the RPE or the choroid for radiation with wavelengths in the 600–800 nm range of wavelengths. For the 200 micron thick choroid, the typical melanosome density is  $5.4 \times 10^9 \text{ cm}^{-3}$ , and with a back scattering coefficient equal to the sum of eqs. [10b] and [11b], this gives an effective mean free path for scattering of an 800 nm photon:

[Para 103]  $\Lambda_{\text{mfp}} = 1/25 = 0.04$  cm, i.e. 400 microns. [12]

[Para 104] This is larger than the thickness of the choroid. The optical density for scattering in the choroid is:

[Para 105]  $OD_{\text{scattering in choroid}} = \mu_{\text{scat}}L_{\text{CH}} = (200/400)(1/2.303) = 0.22$  [13]

[Para 106] This is much less than the optical density for absorption by the melanin. The scattering optical density in the anterior retina is also small.

[Para 107] In the RPE with a normal melanosome density of  $2 \times 10^{10} \text{ cm}^{-3}$ , the mean free path given by eqs. [10a] and [11a] is:

[Para 108]  $\Lambda_{\text{mfp}} = 1/9.54 = 0.01$  cm, i.e. 1000 microns. [14]

[Para 109] This is much larger than the 6–10 micron thickness of the RPE, so the probability that a photon is scattered on traversing the RPE is very small indeed. The optical density for scattering in the RPE is:

[Para 110]  $OD_{\text{scattering in RPE}} = \mu_{\text{scat}}W = 9.54 \times 0.0006/2.303 = 0.004$ . [15]

[Para 111] As in the choroid, this is quite a bit less than the optical density for absorption by the melanin.

[Para 112] Accordingly, in the 600–850 nm range of wavelengths, absorption is more important than scattering both in the RPE and choroid. This then leads to the simple photon transport equations.

[Para 113] We use the simple Kubelka–Munk equations here in order to develop a simple intuition for the dependence of the reflectometry results on the relevant parameters.

[Para 114] Consider first the RPE. The approximate transport equations in the steady state are:

[Para 115]  $dl(+)/dx = -[N(\sigma_s + \sigma_a) + \mu_{\text{back scat}}] I(+)$  +  $[N\sigma_s + \mu_{\text{back scat}}] I(-)$  [16]

[Para 116]  $dl(-)/dy = -[N(\sigma_s + \sigma_a) + \mu_{\text{back scat}}] I(-)$  +  $[N\sigma_s + \mu_{\text{back scat}}] I(+)$  [17]

[Para 117] Here,

- $I(+)$  is the intensity of the input radiation as it travels through the RPE
- $I(-)$  is the intensity of the reflected radiation as it travels backwards through the RPE to the front of the RPE.
- $x$  is the distance into the RPE measured from the front of the RPE
- $y = w - x$ , where  $w$  is the thickness of the RPE melanin layer
- $N$  is the number density of the melanin aggregates that absorb and scatter the radiation
- $\sigma_s$  denotes the cross section of a melanin aggregate for backwards scattering
- $\sigma_a$  denotes the cross section of a melanin aggregate for absorption
- $\mu_{\text{back scat}}$  is the coefficient for backscattering for the structural matrix

[Para 118] It has previously been demonstrated experimentally that  $\sigma_a/(\sigma_s + \sigma_a)$  is quite large, scattering contributing less than 6% to the total optical attenuation across all wavelengths in the UV and optical range.

[Para 119] The quantity  $N(\sigma_s + \sigma_a) w$  is simply 2.303 x the total attenuation (absorption plus scattering) optical density of the RPE melanin layer.

[Para 120] Equations [16] and [17] can be further simplified by ignoring the term  $+ N\sigma_s I(-)$  in eq. [16], the rationale for this being that the reflected signal  $I(-)$  is much smaller than the input signal  $I(+)$ . Then, on requiring that:

[Para 121]  $I(+)$  at  $x = 0$  equals the input intensity  $I_0$  [18a]

[Para 122]  $I(-)$  at  $x = w$  equals  $R_{CH}I(+)$  at  $x = w$  [18b]

[Para 123] where:

- $R_{CH}$  is the reflection coefficient at the interface between the ROE and choroid.

[Para 124] The 10 micron thick blood-rich choriocapillaris does not contain any melanin, and can be ignored in the 600 nm - 750 nm range of wavelengths.

[Para 125] The equations can be solved directly to give for the reflection coefficient  $R_{RPE}$  at  $x = 0$

[Para 126]  $R_{RPE} = I(-)_{at\ x = 0} / I_0$

[Para 127]  $= \{N\sigma_s + \mu_{backscat}\}_{RPE} / \{2N(\sigma_s + \sigma_a) + \mu_{backscat}\}_{RPE}$

[Para 128]  $+ \exp[-2w\{N(\sigma_s + \sigma_a) + \mu_{backscat}\}_{RPE}] [ R_{CH} - \{N\sigma_s + \mu_{backscat}\}_{RPE} / \{2N(\sigma_s + \sigma_a) + \mu_{backscat}\}_{RPE} ]$  [19]

[Para 129] The subscript "RPE" has been added in eq.[19] to indicate that the quantities are for the RPE.

[Para 130] In the same manner, an expression for the reflection coefficient  $R_{CH}$  at the RPE/choroid interface can be obtained:

[Para 131]  $R_{CH} = \{N\sigma_s + \mu_{backscat}\}_{CH} / \{2N(\sigma_s + \sigma_a) + \mu_{backscat}\}_{CH}$

[Para 132]  $+ \exp[-2d_{CH} \{N(\sigma_s + \sigma_a) + \mu_{backscat}\}_{CH}] [ R_{SC} - \{N\sigma_s + \mu_{backscat}\}_{CH} / \{2N(\sigma_s + \sigma_a) + \mu_{backscat}\}_{CH} ]$  [20]

[Para 133] Finally, the total reflection coefficient (at the front of the retina) is given by the same equations to be:

$$[\text{Para 134}] \quad R_{\text{TOT}} = 1 - (1 - R_{\text{RPE}}) \exp[-2 \mu_{\text{back scatRET}} d_{\text{RET}}] \quad [21]$$

[Para 135] where  $\mu_{\text{back scatRET}}$  is the backwards scattering coefficient of the retinal structural matrix.

[Para 136] In these expressions,

- the subscript “CH” has been added to denote that the corresponding quantities are to be evaluated for choroid
- $d_{\text{CH}}$  denotes the thickness of the choroid (200 microns)
- $d_{\text{RET}}$  is the thickness of the anterior retina (200 microns)
- $R_{\text{SC}} = 0.5 \exp[-0.00261(\lambda_{\text{nm}} - 675)]$  denotes the reflection coefficient at the sclera at the back of the choroid.

[Para 137] Insertion of eqs. [19] and [20] into eq. [21] results in the desired overall reflection coefficient.

[Para 138] In the reflectivity, cross-sections for the melanosomes in the RPE and for the melanosomes for the choroid both appear. As indicated above, these melanosomes are quite different. The melanin in the RPE is derived from the neural ectoderm, whereas the choroidal melanin is derived from the neural crest. Melanosomes in the RPE have been found to be different from those in the choroid. In the RPE, the melanosomes are located mainly in the apical region of the RPE cells and are quite elongated in shape, with the long dimension aligned with the apices in order to make close contact with the rods and cones. A typical width for an RPE melanosome has been found to be

approximately 300 nm, whereas the typical length is 720 nm. In the choroid, the melanosomes do not need to be elongated and are primarily globular in shape. The differences in the shapes lead to the differences in the cross-sections as noted above. The melanin sheets stack to form the aggregates in a melanosome, and thus the RPE melanosomes are represented as lossy dielectric prolate spheroids. The globular melanosomes of the choroid are represented by lossy spherical dielectrics.

[Para 139] With respect to numerical results for the eye, the wavelength-dependent quantities in the reflection coefficient are summarized below:

[Para 140] **From the Structural Matrix:**

$$[\text{Para 141}] \quad \mu_{\text{backscatRPE}} = 4.92 \times 10^{-6} \lambda_{\text{nm}}^2 \text{ cm}^{-1} \quad [22\text{a}]$$

$$[\text{Para 142}] \quad \mu_{\text{backscatRPE}} = 4.92 \times 10^{-6} \lambda_{\text{nm}}^2 \text{ cm}^{-1} \quad [22\text{b}]$$

$$[\text{Para 143}] \quad \mu_{\text{backscatCH}} = 3.76 \times 10^{-5} \lambda_{\text{nm}}^2 \text{ cm}^{-1} \quad [23]$$

[Para 144] **Melanin Related:**

$$[\text{Para 145}] \quad \sigma_{\text{sRPE}} = 0.03 \times 10^{-14} \lambda_{\text{nm}}^2 \text{ cm}^2 \quad [24]$$

$$[\text{Para 146}] \quad \sigma_{\text{sCH}} = 0.05 \times 10^{-10} \lambda_{\text{nm}}^2 \text{ cm}^2 \quad [25]$$

$$[\text{Para 147}] \quad \sigma_{\text{a}} = 9.47 \times 10^{-7} \exp[-0.0062 \lambda_{\text{nm}}] \text{ cm}^2 \quad [26]$$

$$[\text{Para 148}] \quad N_{\text{RPE}} = 2 \times 10^{10} \text{ cm}^{-3} \text{ for a normal patient} \quad [27\text{a}]$$

$$[\text{Para 149}] \quad N_{\text{CH}} = 5.4 \times 10^9 \text{ cm}^{-3} \text{ for a normal patient} \quad [27\text{b}]$$

[Para 150] **Relevant Dimensions:**

$$[\text{Para 151}] \quad w = 0.0006 \text{ cm} \quad [28\text{a}]$$

$$[\text{Para 152}] \quad d_{\text{CH}} = 0.0200 \text{ cm} \quad [28\text{b}]$$

[Para 153] It is interesting that eq. [23] for the reflectivity depends on only the five parameter combinations:

[Para 154]  $\{\sigma_s/2(\sigma_s + \sigma_a)\}_{CH}$

[Para 155]  $\{\sigma_s/2(\sigma_s + \sigma_a)\}_{RPE}$

[Para 156]  $\exp[-2\mu_{backscatRET}) d_{RET}]$

[Para 157]  $\exp[-2\{N(\sigma_s + \sigma_a)\}_{RPE} + \mu_{backscatRPE}) w]$

[Para 158]  $\exp[-2\{N(\sigma_s + \sigma_a)\}_{CH} + \mu_{backscatCH}) d_{CH}]$

[Para 159] The fourth (exponential) parameter combination provides the desired sensitive measure of the RPE melanin concentration  $N_{RPE}$ .

[Para 160] FIGURES 8–15 are graphs providing the implications of equations [19]–[21], and particularly equation [21] for the overall reflectivity of the anterior retina, RPE and choroid. They display variations in the parameters with wavelengths, RPE and choroid melanosome number densities.

[Para 161] With reference to FIG. 8, a comparison of RPE melanin absorption coefficient (top curve), RPE melanin scattering coefficient (middle curve) and RPE structural matrix scattering coefficient (bottom curve) is shown. The logs (to the base 10) of the coefficients are shown, with the coefficients expressed in  $\text{cm}^{-1}$ . The logarithms are plotted versus wavelengths and nanometers between 600 nm and 800 nm. A normal RPE melanosome concentration of  $2 \times 10^{10} \text{cm}^{-3}$  has been assumed. FIG. 8 shows that in the RPE at normal melanosome densities, the absorption coefficient is largest followed by the scattering coefficient due to the melanin and the scattering coefficient of the structural

matrix. A drastic reduction in the melanosome density would have to occur before the scattering coefficients become as large as the absorption coefficient.

[Para 162] With reference now to FIG. 9, a comparison of choroid melanin absorption coefficient (top curve), choroid melanin scattering coefficient (bottom curve), and choroid structural matrix scattering coefficient (middle curve) is shown. The logs (to the base 10) of the coefficients are shown, with the coefficients expressed in  $\text{cm}^{-1}$ . The logarithms are plotted vs wavelengths in nanometers between 600 nm and 800 nm. A normal choroid melanosome concentration of  $5.4 \times 10^9 \text{ cm}^{-3}$  has been assumed in these plots. In the choroid at normal melanosome densities, the absorption coefficient due to the melanosomes is the largest, followed by the scattering coefficient from the structural matrix, with a much smaller scattering coefficient from the melanosomes. However, the difference between the melanosome absorption coefficient and the matrix scattering coefficient is small at 800 nm. If the choroid melanosome density decreases, the matrix scattering coefficient can become larger than the melanosome absorption coefficient. This is especially true at wavelengths near 800 nm.

[Para 163] As seen from eqs. [19]–[21], the total reflectivity is determined by the reflectivities of the RPE and of the choroid, i.e. by  $R_{\text{RPE}}$  and  $R_{\text{CH}}$ . These are shown in FIGS. 10 and 11.

[Para 164] FIGURE 10 is a graph illustrating reflectivity  $R_{\text{CH}}$  of choroid (top curve) as a function of wavelength (in nm), at a normal choroid melanosome density ( $5.4 \times 10^9 \text{ cm}^{-3}$ ). Two other curves are also shown, one for each of the

components of eq. [20] comprising the expression for  $R_{CH}$ . The middle curve is the fractional term containing the choroid scattering coefficients in the numerator and the sum the of the scattering and absorption coefficients in the denominator. The bottom curve is the exponential term with its factor. FIG. 10 shows that the reflectivity increases as the wavelength increases. This results from the increase in the (backwards) scattering coefficient with wavelength in the Mie regime of scattering. By far the dominant contribution to the reflectivity of the choroid at normal choroid melanosome densities is the fraction containing the ratios of the scattering and absorption coefficients. The exponential term is quite negligible.

[Para 165] FIGURE 11 is a graph depicting reflectivity  $R_{RPE}$  of RPE (top curve) as a function of wavelength (in nm), at normal RPE and choroid melanosome densities ( $2 \times 10^{10} \text{ cm}^{-3}$  and  $5.4 \times 10^9 \text{ cm}^{-3}$ , respectively). Two other curves are also shown, one for each of the components of eq. [19] comprising the expression for  $R_{RPE}$ . The middle curve is the fractional term containing the RPE scattering coefficients in the numerator and the sum the of the scattering and absorption coefficients in the denominator. The bottom curve is the exponential term with its factor that contains  $R_{CH}$ . FIG. 11 shows that the reflectivity increases as the wavelength increases, just as with the reflectivity from the choroid. Again, this results from the increase in the (backwards) scattering coefficient with wavelength in the Mie regime of scattering. By far the dominant contribution to the reflectivity of the RPE at normal RPE and choroid melanosome densities is the fraction containing the ratios of the RPE

scattering and absorption coefficients. The exponential term is much smaller, due to the large RPE absorption coefficient due to the melanosomes.

[Para 166] FIGURE 12 illustrates that equation [21] shows how the total reflectivity  $R_{TOT}$  is derived from the reflectivity of the RPE  $R_{RPE}$ , contains an exponential attenuation factor that contains the extinction coefficient due to scattering in the anterior retina. FIG. 12 illustrates the transmission factor of the anterior retina as given by the exponential factor of equation [21] versus the wavelength in nanometers. The transmission of the reflected radiation through the anterior retina is quite good, varying from 93+% at 600 nm to 88+% at 800 nm.

[Para 167] It should be noted that the RPE melanin concentration varies with lateral position in the eye. It peaks at the center of the macula and then decreases on either side over a range of approximately  $5^\circ$  to a relatively constant value for about  $10^\circ$  on either side, before rising again towards the equator at  $-20^\circ$  and  $+15^\circ$ . To get consistent results, it is best to operate the detector 110, preferably a reflectometer in accordance with the present invention, in the regions where the concentration is relatively constant, or in other words on the order of approximately  $10^\circ$  away from the center of the macula.

[Para 168] The foregoing figures, including FIGS. 5-12, show the behavior at normal RPE and normal choroid melanosome densities ( $2 \times 10^{10} \text{cm}^{-3}$  and  $5.4 \times 10^9 \text{cm}^{-3}$  respectively) The present invention is particularly interested in

how the total reflectivity  $R_{TOT}$  changes as the RPE melanosomes densities change. This is illustrated and described in connection with FIGS. 13–15.

[Para 169] FIGURE 13 illustrates the percentage changes in the total reflectivity  $R_{TOT}$  as a function of wavelength in nanometers, as RPE and choroid melanosome densities vary from the normal  $n_{RPE} = 2 \times 10^{10} \text{ cm}^{-3}$  and  $n_{CH} = 5.4 \times 10^9 \text{ cm}^{-3}$ . Four curves are shown. The top curve is for a normal RPE density and a choroid density that is 1/6 normal ( $n_{RPE}$  and  $(1/6) n_{CH}$ ). The upper middle curve is for  $(1/6) n_{RPE}$  and  $n_{CH}$ . The lower middle curve is for  $n_{RPE}$  and  $6n_{CH}$ . The lowest curve (at 600 nm) is for  $6n_{RPE}$  and  $n_{CH}$ . FIG. 13 shows that comparable percentage changes occur in  $R_{TOT}$  from comparable changes in RPE melanosome densities and in choroid melanosome densities, but that the changes from RPE densities have a different wavelength dependence from changes in choroid densities. Accordingly, measurements of the percentage changes in the total reflectivity at two different wavelengths can uniquely determine what the changes in RPE and choroid melanosome densities are.

[Para 170] The use of dual-wavelength reflectometry to determine both the RPE melanosomes density or concentration and the choroid melanosome density or concentration is further illustrated in FIGS. 14 and 15. FIGS. 14 and 15 are contour plots of percentage change in the total reflectivity as a function of  $r = n_{RPE}(\text{abnormal}) / n_{RPE}(\text{normal})$  on the abscissa (x-axis) and  $c = n_{CH}(\text{abnormal}) / n_{CH}(\text{normal})$  on the ordinate (y-axis). FIG. 14 shows the plot at 600 nm, and FIG. 15 shows the plot at 800 nm. It is apparent that the percentage change contours at 600 nm have a different shape than the

contours at 800 nm. A given percentage change at 600 nm and another given percentage change at 800 nm then provide two different contours, and the intersection of these two contours provides uniquely the abnormal melanosome densities for both the RPE and the choroid. One way to solve the expressions for the unique RPE and choroid melanosome densities that give the measured reflectivities at the two wavelengths may be simply to store in computer memory a look-up table of the reflectivity contours at two different wavelengths in the 600–800 nm range of wavelengths, and to look for the two contours corresponding to the measurements to find the one common pair of RPE and choroid densities. Alternatively, the pertinent equations above can be solved, such as using a computer or other electronic device.

[Para 171] The curves in the figures herein have been generated with approximate expressions, so the absolute magnitudes of the reflection coefficient shown (of the order of a few percent) should be taken as estimates of the actual reflection coefficient. The actual value will depend upon the specifics of the detectors optics and geometry. A baseline may be established from a population of normal patients, from which deviations can be established. Thus, FIGS. 14 and 15 show percentage change contours for abnormalities rather than absolute value contours of the reflectivity.

[Para 172] Table 1 below shows the peak laser power that will maintain the Arrhenius integral for HSP activation at a conservative value of unity when the RPE melanin content takes on different values. Peak power for different values of spot radius, train duration, duty cycle and abnormal RPE melanin ratio

content is shown. The table assumes a treatment pulsed wavelength at 810 nm.

[Para 173] TABLE 1:

R(micron)	tF (sec)	dc (%)	$\alpha/\alpha_{normal}$		Psdm(watts)
100	0.2	2	1		3.44
			3		3.14
			5		0.69
			8		0.43
100	0.2	3	1		2.29
			3		0.76
			5		0.46
			8		0.29
100	0.2	4	1		1.72
			3		0.57
			5		0.34
			8		0.21
100	0.2	5	1		1.38
			3		0.46
			5		0.28
			8		0.17
100	0.3	2	1		2.68
			3		0.89
			5		0.54
			8		0.33
100	0.3	3	1		1.79
			3		0.6
			5		0.36
			8		0.22

100	0.3	4	1		1.34
			3		0.45
			5		0.27
			8		0.17
100	0.3	5	1		1.07
			3		0.36
			5		0.21
			8		0.14
100	0.4	2	1		2.14
			3		0.71
			5		0.43
			8		0.27
100	0.4	3	1		1.43
			3		0.48
			5		0.29
			8		0.18
100	0.4	4	1		1.07
			3		0.36
			5		0.21
			8		0.13
100	0.4	5	1		0.86
			3		0.29
			5		0.17
			8		0.11
100	0.5	2	1		1.72
			3		0.57
			5		0.34
			8		0.21

100	0.5	3	1		1.15
			3		0.38
			5		0.23
			8		0.14
100	0.5	4	1		0.86
			3		0.29
			5		0.17
			8		0.11
100	0.5	5	1		0.69
			3		0.23
			5		0.14
			8		0.09
200	0.2	2	1		6.88
			3		2.29
			5		1.38
			8		0.86
200	0.2	3	1		4.59
			3		1.53
			5		0.92
			8		0.57
200	0.2	4	1		3.44
			3		1.15
			5		0.69
			8		0.43
200	0.2	5	1		2.75
			3		0.92
			5		0.55
			8		0.34

200	0.3	2	1		5.36
			3		1.79
			5		1.07
			8		0.67
200	0.3	3	1		3.57
			3		1.19
			5		0.71
			8		0.45
200	0.3	4	1		2.68
			3		0.89
			5		0.54
			8		0.33
200	0.3	5	1		2.14
			3		0.71
			5		0.43
			8		0.27
200	0.4	2	1		4.28
			3		1.43
			5		0.86
			8		0.54
200	0.4	3	1		2.85
			3		0.95
			5		0.57
			8		0.36
200	0.4	4	1		2.14
			2		0.71
			5		0.43
			8		0.27

200	0.4	5	1		1.71
			3		0.57
			5		0.34
			8		0.21
200	0.5	2	1		3.44
			3		1.15
			5		0.69
			8		0.43
200	0.5	3	1		2.3
			3		0.77
			5		0.28
			8		0.29
200	0.5	4	1		1.72
			3		0.57
			5		0.34
			8		0.22
200	0.5	5	1		1.38
			3		0.46
			5		0.28
			8		0.17

[Para 174] As shown in Table 1 above, the range of the ratio of abnormal RPE melanin content to normal RPE melanin content has been taken to a range between one and eight. The peak laser power depends on the laser spot radius at the retina, the duration of the micropulse train and the duty cycle. For each of these cases, the ratio of abnormal to normal RPE melanin content has been taken to be one, three, five and eight.

[Para 175] Any abnormal RPE melanin content manifests itself through a change in the absorption coefficient of the RPE to the incoming laser radiation: the absorption coefficient is proportional to the total RPE melanin content. Accordingly, in the table, RPE melanin content is represented by 4 values of the ratio of the absorption coefficient  $\alpha$  to the normal absorption coefficient  $\alpha_{\text{normal}}$ :

[Para 176]  $\alpha/\alpha_{\text{normal}} = 1, 3, 5, 8.$

[Para 177] The effect of melanin content on the peak laser treatment power  $P_{\text{sdm}}$  depends on the laser's retinal spot radius (R), the duration of the micropulse train ( $t_F$ ), and the duty cycle (dc) of the micropulse train ( $t_F$ ). In the table, examples are given for  $P_{\text{sdm}}$  (in watts) for all possible combinations of:

[Para 178]  $R = 100$  microns,  $200$  microns

[Para 179]  $t_F = 0.2$  sec,  $0.3$  sec,  $0.4$  sec, and  $0.5$  sec

[Para 180]  $dc = 2\%$ ,  $3\%$ ,  $4\%$ ,  $5\%$

[Para 181] for each of the 4 values of the ratio  $\alpha/\alpha_{\text{normal}}$ .

[Para 182] The value of  $\lambda_{\text{nm}}$  shown is the value of the peak power that maintains the Arrhenius integral for heat shock protein (HSP) activation  $\Omega_{\text{hsp}}$  at a (conservative) treatment value of unity:

[Para 183]  $\Omega_{\text{hsp}} = 1.$

[Para 184] And it has been assumed that the treatment laser wavelength is  $810$  nm - for which  $\alpha_{\text{normal}} = 104 \text{ cm}^{-1}$ .

[Para 185] For an arbitrary near-IR wavelength (in nanometers)  $\lambda_{\text{nm}}$ , the treatment powers in the table should be multiplied by the factor  $\xi(\lambda_{\text{nm}})$ :

[Para 186]  $\xi(\lambda_{\text{nm}}) = \text{Exp}[0.0062(810 - \lambda_{\text{nm}})]$

[Para 187] i.e.

[Para 188]  $P_{sdm}(\lambda_{nm}) = P_{sdm} \xi(\lambda_{nm}) = P_{sdm} \text{ (table value)} \times \text{Exp}[0.0062(810 - \lambda_{nm})]$ .

[Para 189] From the foregoing, it can be seen that  $P_{sdm}$  decreases as  $\alpha/\alpha_{normal}$  increases; the values of  $P_{sdm}$  are larger the larger the spot radius (R) is; the values of  $P_{sdm}$  are larger the smaller the train duration  $t_F$  is; and the values of  $P_{sdm}$  are larger the smaller the duty cycle (dc) is.

[Para 190] FIGURES 16 and 17 are graphs that show the ratio  $r_{damage}$  of abnormal RPE melanin content to normal RPE melanin content at which damage can occur. These graphs are based on rough approximate expressions for the Arrhenius integrals for HSP activation and for damage that give surprisingly close matches to the exact expressions. Both graphs plot the ratio  $r_{damage}$  vs the pulse train duration  $t_F$ . The graph of FIG. 16 covers the range of  $t_F$  from 0.01 sec to 1 sec. The graph of FIG. 17 covers a more realistic clinical range of  $t_F$  from 0.2 to 0.5 sec.

[Para 191] As can be seen in FIGS. 16 and 17, the critical ratio  $r_{damage}$  of abnormal RPE melanin content to normal RPE melanin content at which damage can occur varies from 4 to about 8 for pulse train durations ranging from 0.2 sec to 0.5 sec. Thus, one or more treatment parameters, as described above, are adjusted when the content of melanin in the RPE is determined to be at least four times greater than a normal content of melanin in the RPE. Thus, assuming a normal RPE density of  $2 \times 10^{10} \text{ cm}^{-3}$ , the one or more treatment parameters are adjusted when the content of melanin in the RPE is determined to be greater than  $8 \times 10^{10} \text{ cm}^{-3}$ .

[Para 192] At this critical ratio, damage can be avoided and effective HSP activation can be assured, by changing the treatment parameters from their normal values. For example, for most clinical treatment parameters of interest:

[Para 193] The peak power  $P$  can be reduced from its normal value  $P_{\text{normal}}$  to lie in the range

[Para 194]  $P_{\text{normal}} / r_{\text{damage}} < P < P_{\text{normal}}$

[Para 195] if the duty cycle and retinal spot radius are left at their normal values.

[Para 196] The duty cycle  $dc$  can be reduced from its normal value  $dc_{\text{normal}}$  to lie in the range

[Para 197]  $dc_{\text{normal}} / r_{\text{damage}} < dc < dc_{\text{normal}}$

[Para 198] if the laser peak power and retinal spot radius are left at their normal values

[Para 199] The retinal spot radius  $R$  can be increased from its normal value  $R_{\text{normal}}$  to lie in the range

[Para 200]  $R_{\text{normal}} < R < R_{\text{normal}} / r_{\text{damage}}$

[Para 201] if the laser peak power and duty cycle are left at their normal values.

[Para 202] Although a single laser phototherapy parameter may be adjusted, it will be understood that more than one of these parameters can also be adjusted simultaneously. For example, the laser spot radius can be increased in diameter and the power lessened, but not lessened to the extent it would otherwise require if only the power were lessened. Similarly, all of the

parameters can be adjusted slightly, such as slightly increasing the retinal spot size for the treatment light beam, lowering the pulse train duration of the treatment light beam, lowering the duty cycle of the treatment light beam, and lowering the power of the treatment light beam such that unity in the Arrhenius integral is achieved in order to avoid damage to the retina and eye of the patient having an abnormally large concentration or amount of melanin in his or her RPE.

[Para 203] Although several embodiments have been described in detail for purposes of illustration, various modifications may be made without departing from the scope and spirit of the invention. Accordingly, the invention is not to be limited, except as by the appended claims.

**What is claimed is:**

**[Claim 1]** A process for safely providing retinal phototherapy, comprising the steps of:

generating a first light beam and a second light beam each having a wavelength between 550nm and 900nm, wherein the first and second light beams have a different wavelength;

applying the first and second light beams to a retinal pigment epithelium and a choroid of an eye;

measuring the amount of light reflected from the retinal pigment epithelium and the choroid by the first beam and the second light beam;

determining a content of melanin within the retinal pigment epithelium of the eye using the measured amount of light reflected from the retinal pigment epithelium and the choroid of the eye from the first and second light beams;  
and

adjusting one or more treatment parameters of the retinal phototherapy if the content of melanin in the retinal pigment epithelium of the eye exceeds a predetermined amount.

**[Claim 2]** The process of claim 1, wherein the measuring step comprises using a reflectometer to measure the amount of light reflected from the retinal pigment epithelium and the choroid of the eye from the first and second light beams.

[Claim 3] The process of claim 1, wherein the first and second light beams differ in wavelength by at least 25nm.

[Claim 4] The process of claim 1, wherein the first and second light beams each have a wavelength between 600nm and 850nm.

[Claim 5] The process of claim 1, including the step of distinguishing the amount of light reflected by the first and second light beams from the retinal pigment epithelium and the choroid.

[Claim 6] The process of claim 1, wherein the adjusting step comprises adjusting at least one of a retinal spot size of a treatment light beam, a pulse train duration of the treatment light beam, a duty cycle of the treatment light beam, or a power of the treatment light beam.

[Claim 7] The process of claim 1, wherein the adjusting step comprises increasing a retinal spot size of a treatment light beam.

[Claim 8] The process of claim 1, wherein the adjusting step comprises lowering a pulse train duration of a treatment light beam.

[Claim 9] The process of claim 1, wherein the adjusting step comprises lowering a duty cycle of a treatment light beam.

[Claim 10] The process of claim 1, wherein the adjusting step comprises lowering a power of a treatment light beam.

[Claim 11] The process of claim 1, including the step of automatically adjusting one or more treatment parameters of a retina therapy system when the content of melanin in the retinal pigment epithelium of the eye exceeds the predetermined amount.

[Claim 12] The process of claim 11, including the step of notifying of the one or more retinal treatment parameters that is adjusted.

[Claim 13] The process of claim 1, wherein the one or more treatment parameters are adjusted when the content of melanin in the retinal pigment epithelium of the eye is determined to be at least four times greater than a normal content of melanin in the retinal pigment epithelium.

[Claim 14] The process of claim 1, wherein the one or more treatment parameters are adjusted when the content of melanin in the retinal pigment epithelium of the eye is determined to be greater than  $8 \times 10^{10} \text{ cm}^{-3}$ .

[Claim 15] A process for safely providing retinal phototherapy, comprising the steps of:

generating a first light beam and a second light beam each having a wavelength between 550nm and 900nm, wherein the first and second light beams have a different wavelength;

applying the first and second light beams to a retinal pigment epithelium and a choroid of an eye;

using a reflectometer to measure the amount of light reflected from the retinal pigment epithelium and the choroid by the first and second light beams;

determining a content of melanin within the retinal pigment epithelium of the eye using the measured amount of light reflected from the retinal pigment epithelium and the choroid of the eye from the first and second light beams;  
and

adjusting one or more treatment parameters of a pulsed light beam retina therapy if the content of melanin in the retinal pigment epithelium of the eye is determined to be four to eight times a normal melanin content of the retinal pigment epithelium of the eye for pulse train durations of the pulsed light beam retina therapy ranging from 0.2 to 0.5 seconds.

[Claim 16] The process of claim 15, wherein the adjusting step includes the step of enlarging treatment light beam retinal spot size, lowering treatment light beam power, lowering treatment light beam duty cycle, or lowering treatment light beam pulse train duration.

[Claim 17] The process of claim 15, wherein the first and second light beams differ in wavelength by at least 25nm.

[Claim 18] The process of claim 17, wherein the first and second light beams each have a wavelength between 600nm and 850nm.

[Claim 19] The process of claim 15, including the step of distinguishing the amount of light reflected by the first and second light beams from the retinal pigment epithelium and the choroid.

[Claim 20] The process of claim 16, including the step of automatically adjusting one or more treatment parameters of a retina therapy system when the concentration of melanin in the retinal pigment epithelium of the eye exceeds the predetermined amount.

[Claim 21] The process of claim 20, including the step of notifying of the one or more retinal treatment parameters that is adjusted.

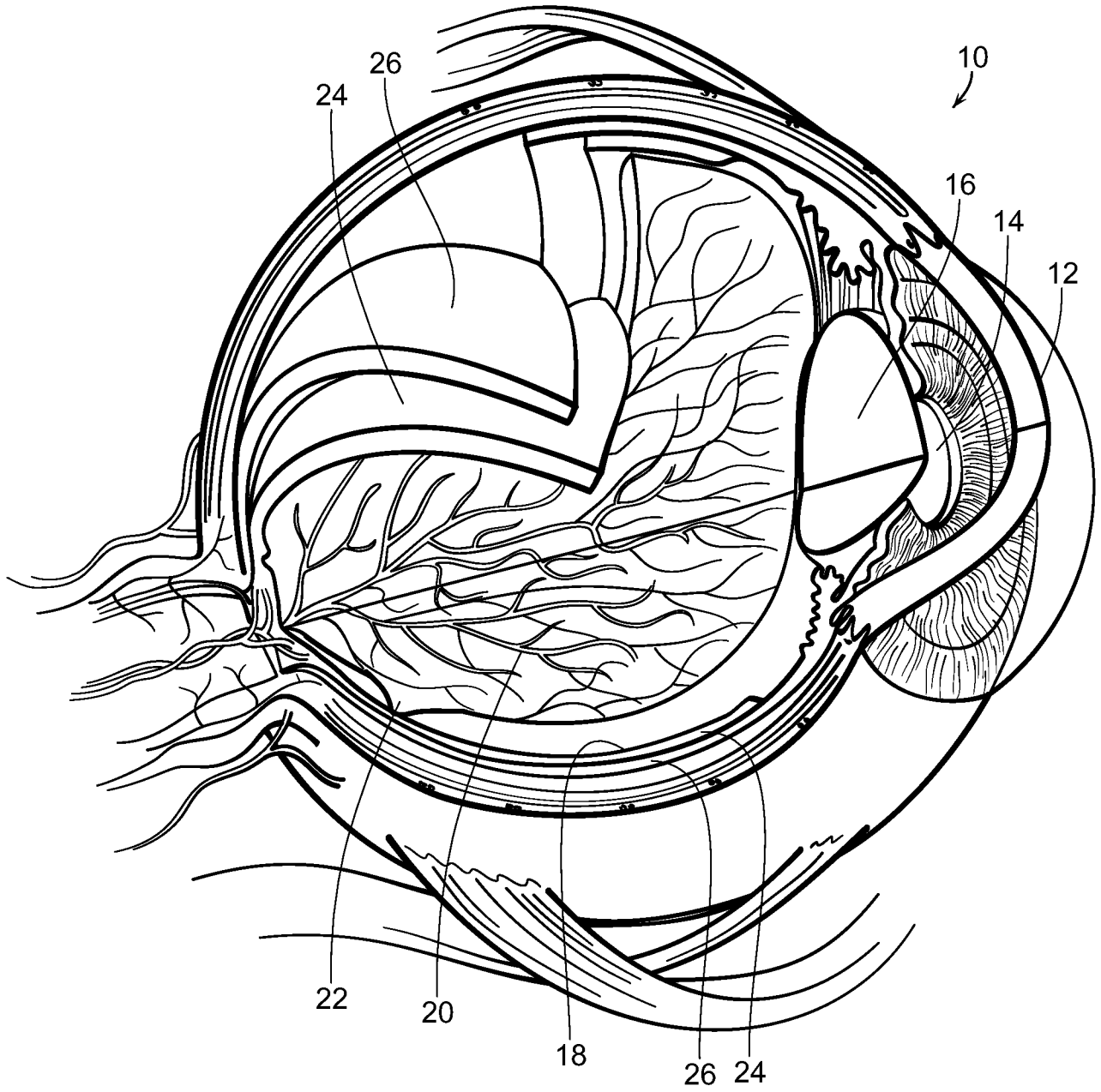


FIG. 1

2/11

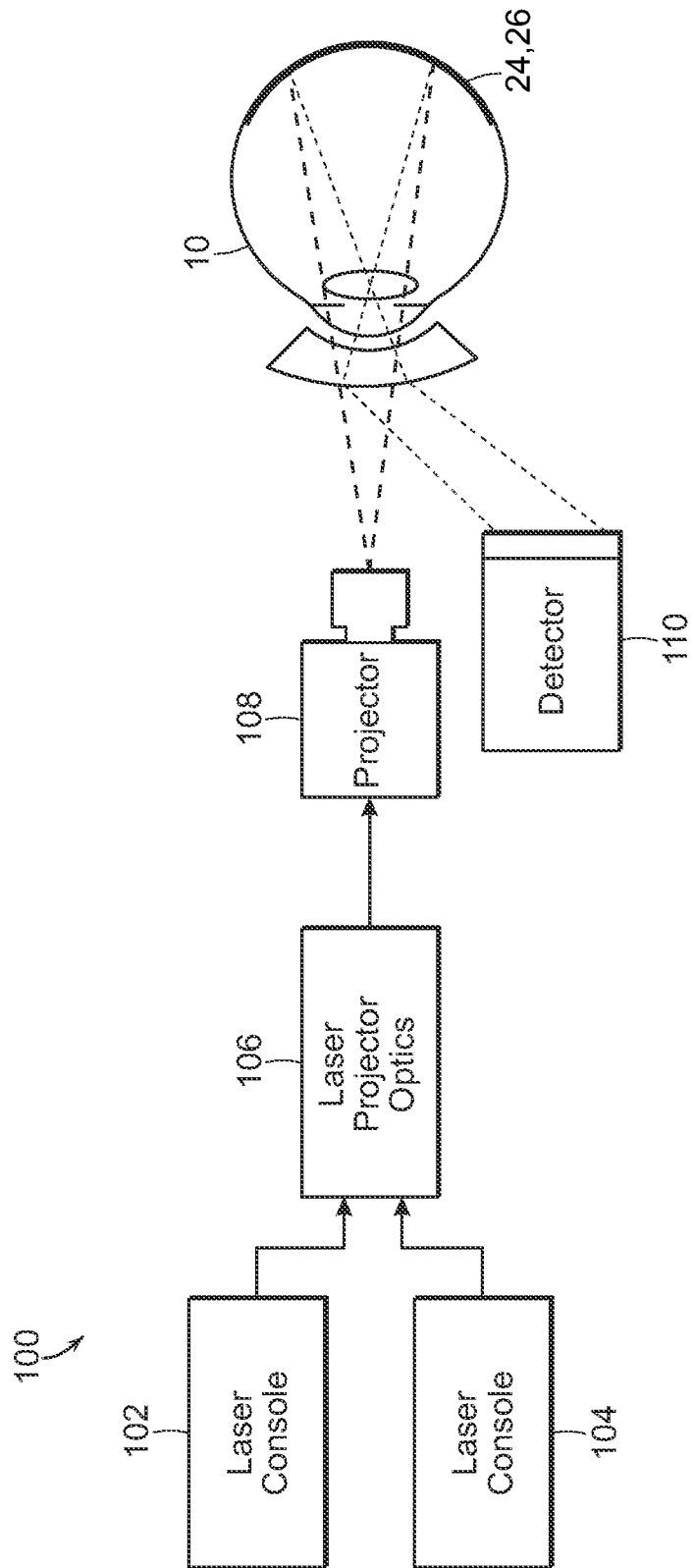


FIG. 2

3/11

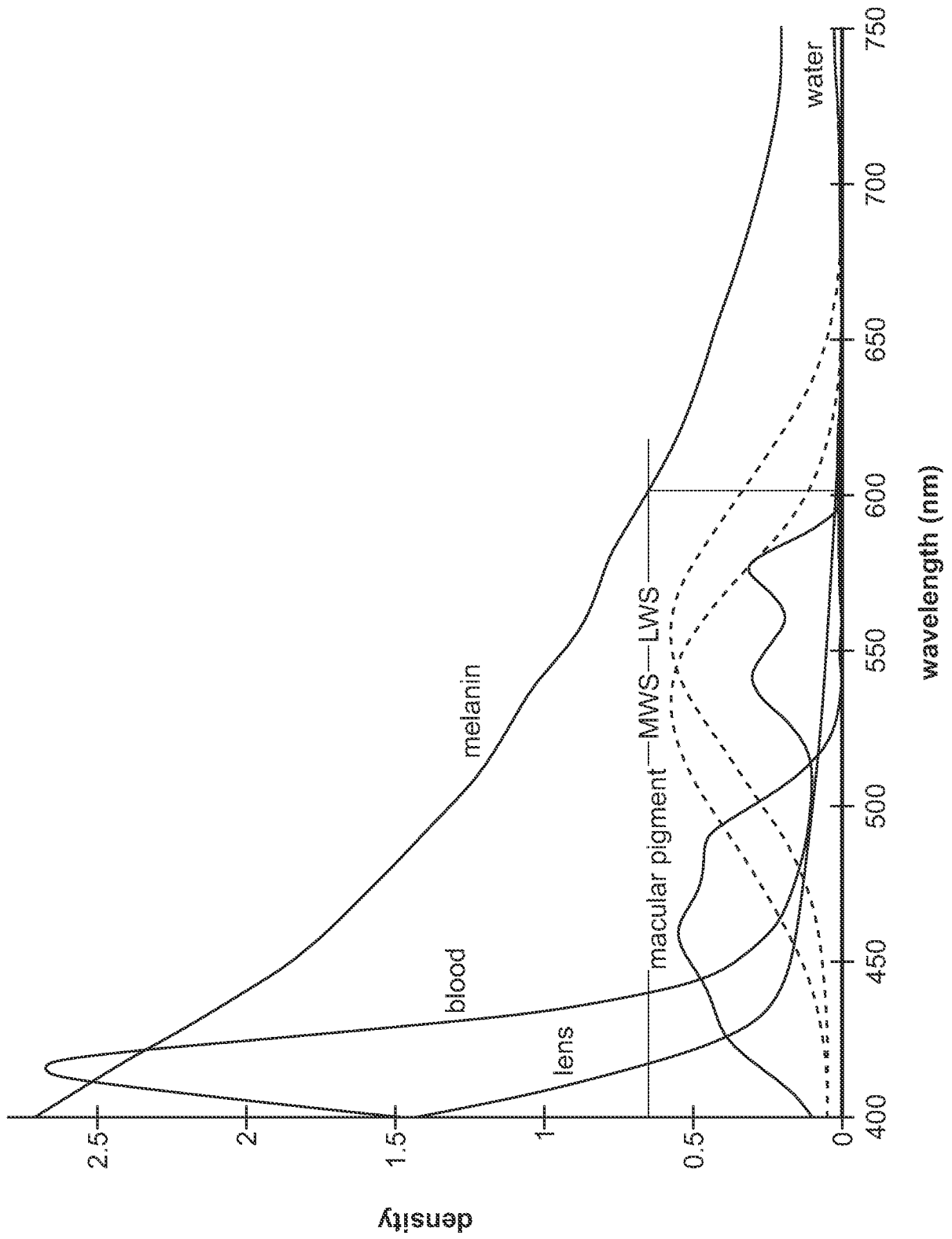


FIG. 3

4/11

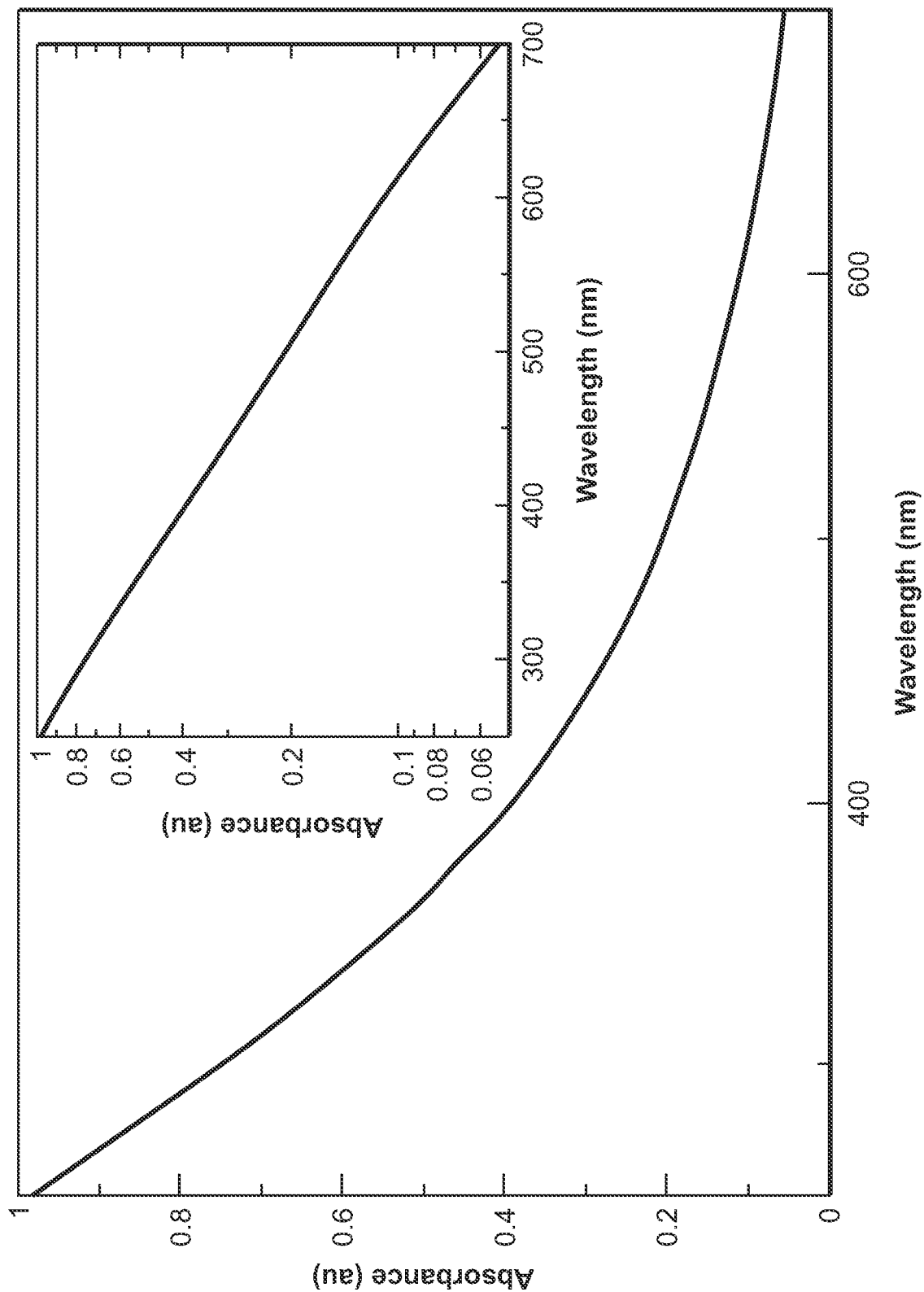


FIG. 4

5/11

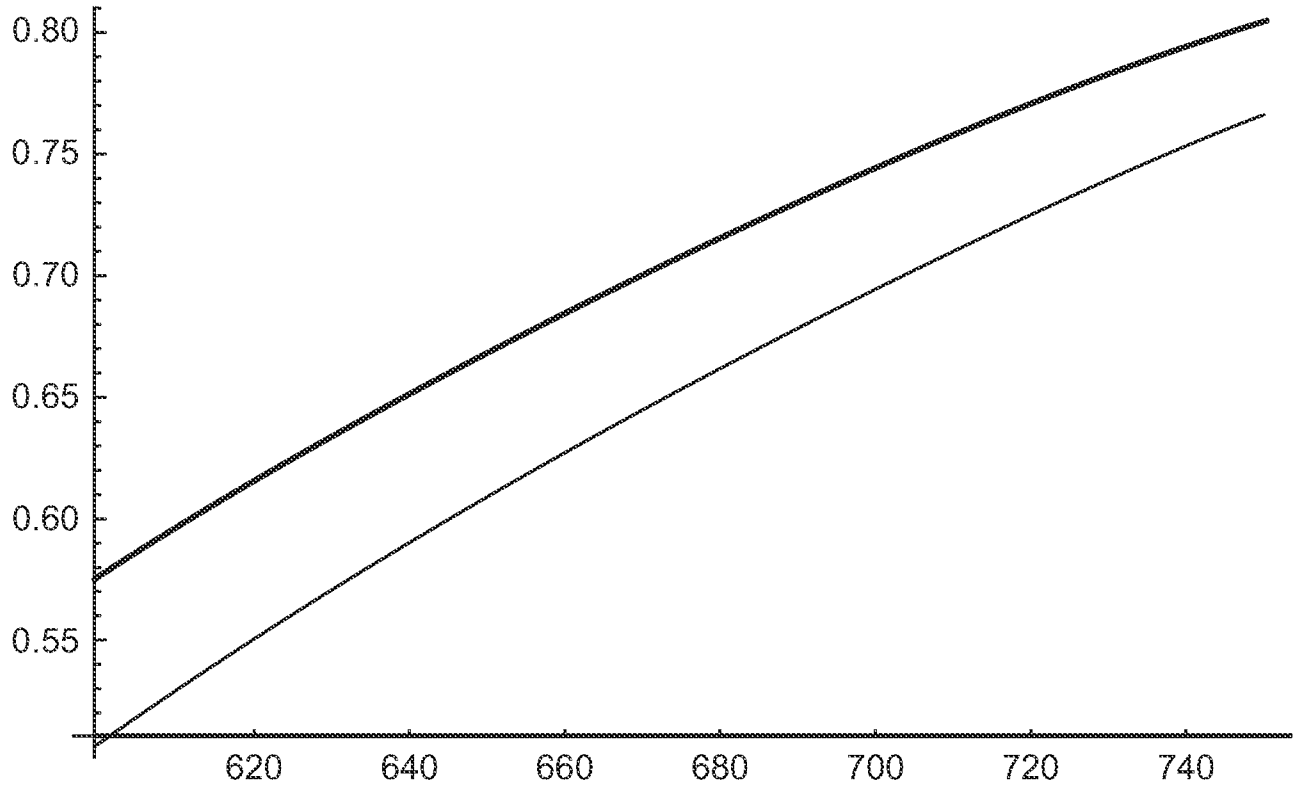


FIG. 5

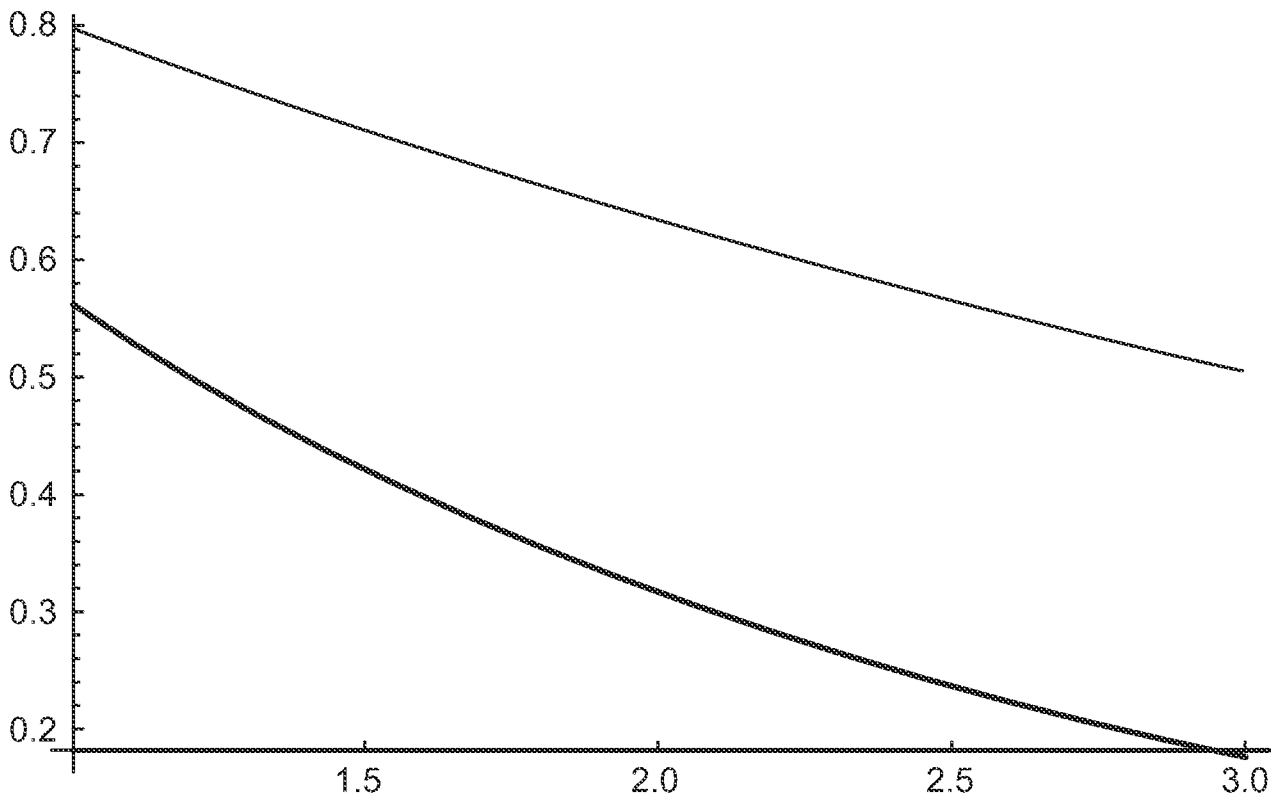
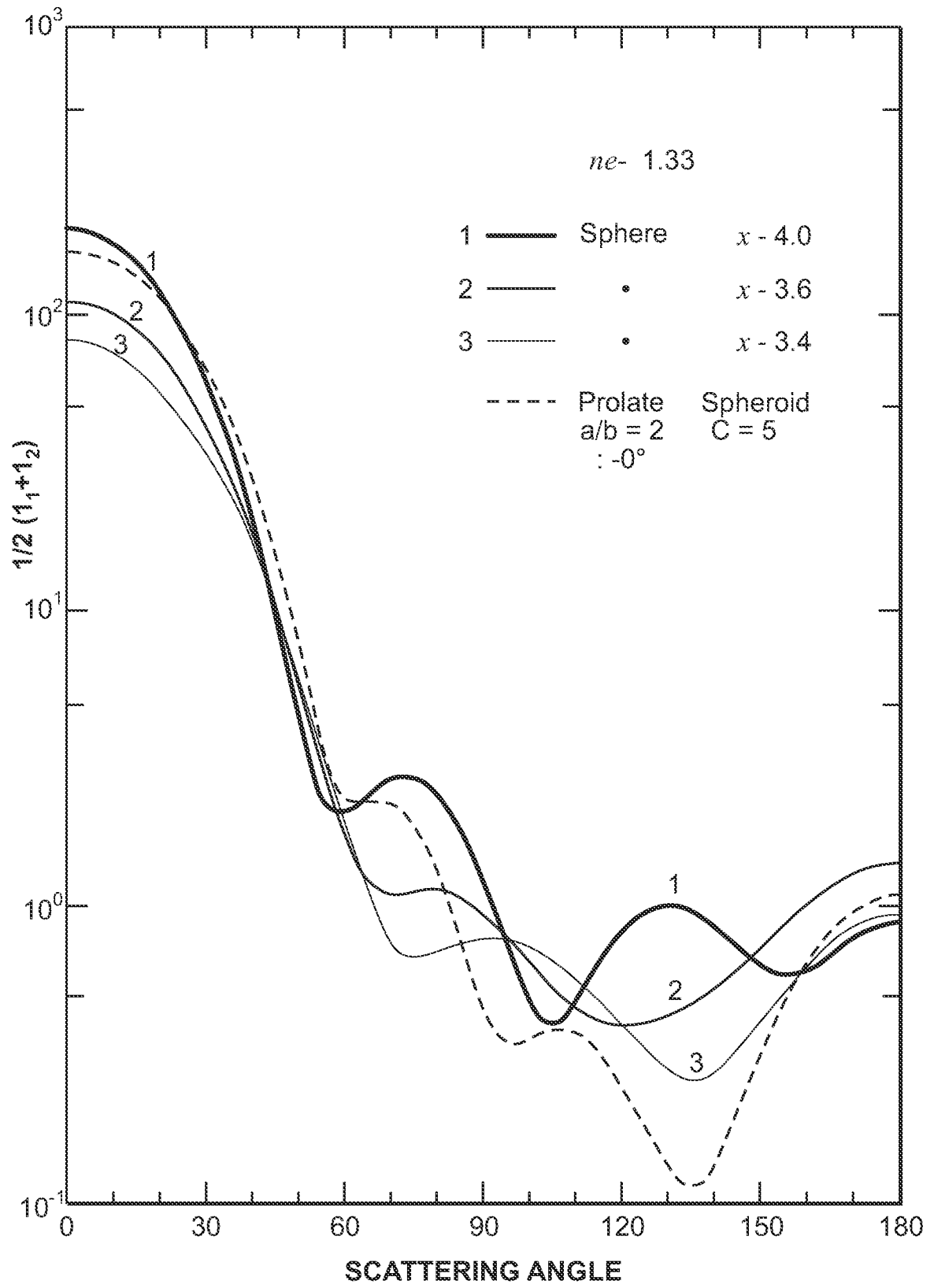


FIG. 6

6/11



7/11

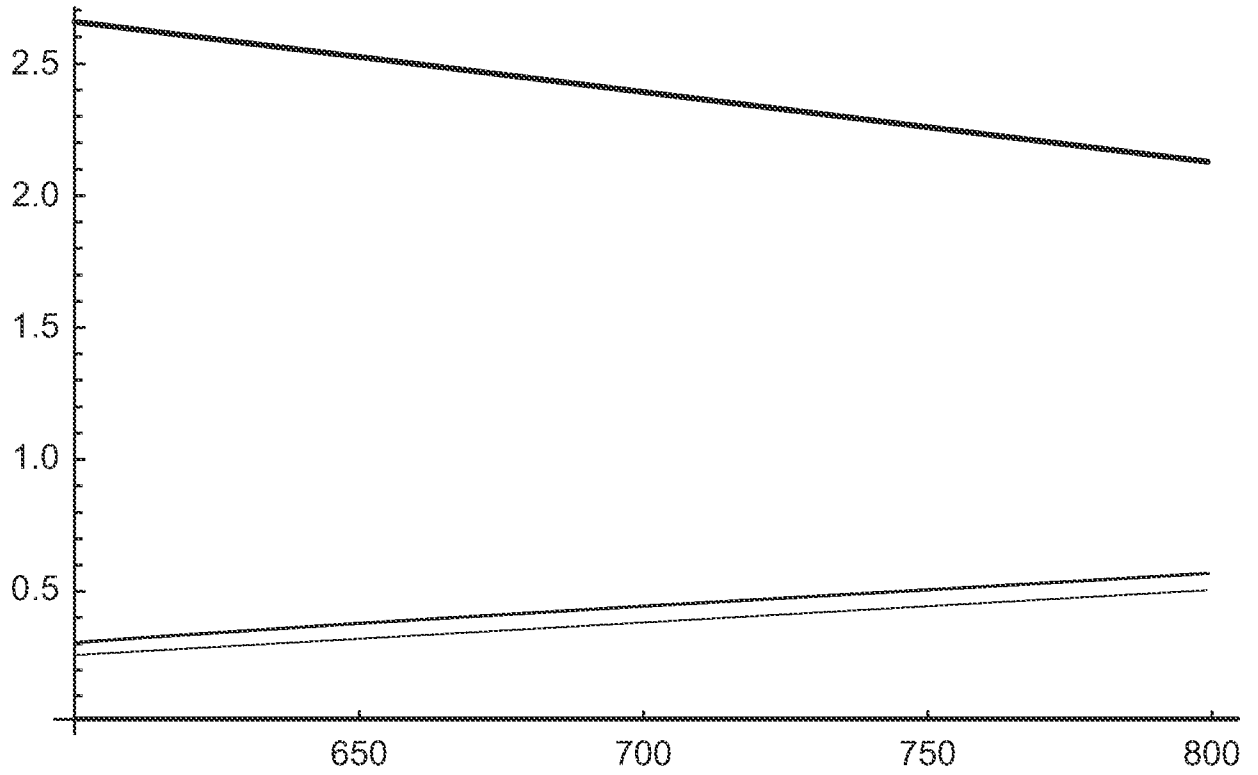


FIG. 8

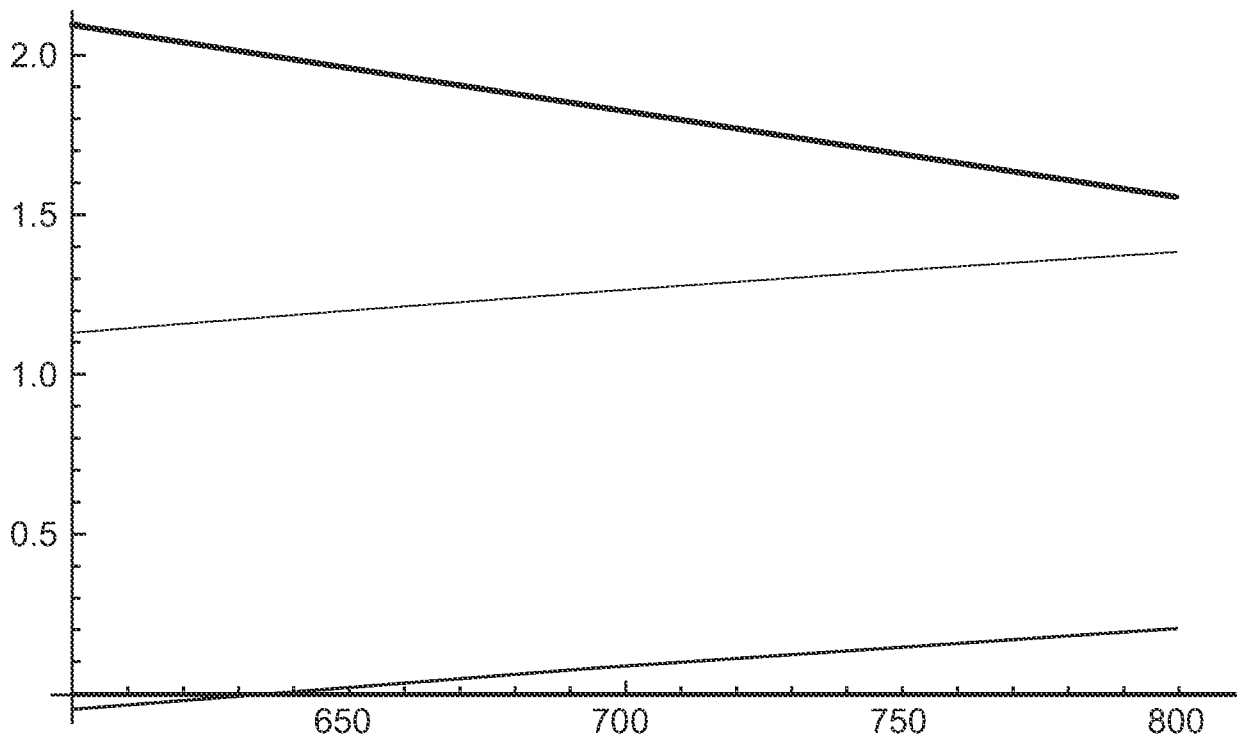


FIG. 9

8/11

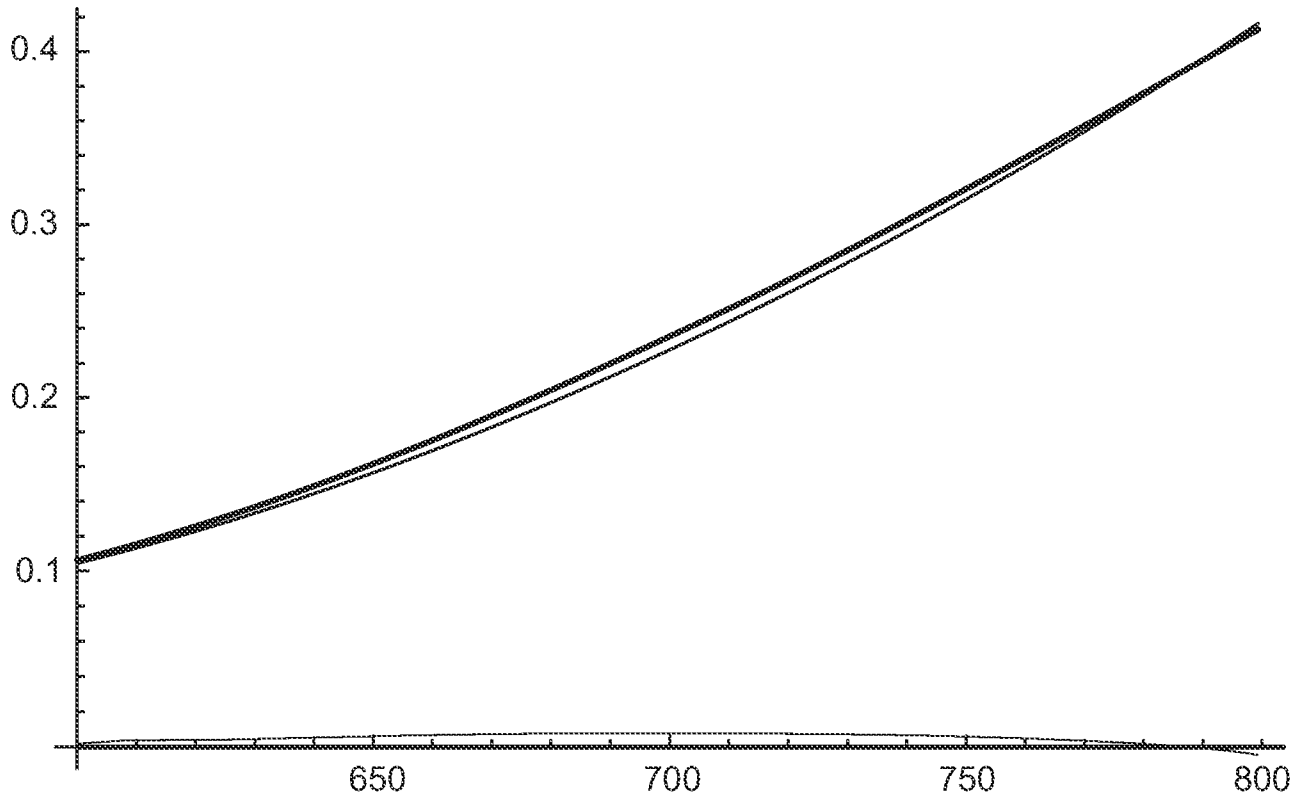


FIG. 10

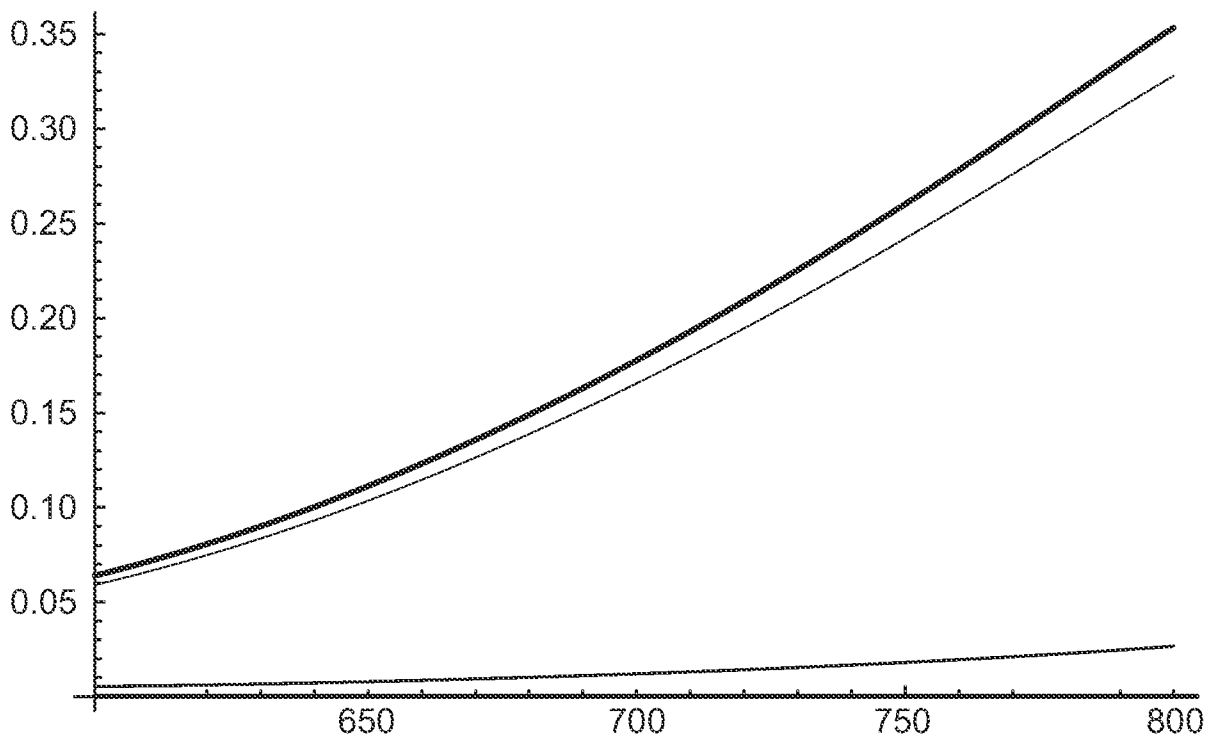


FIG. 11

9/11

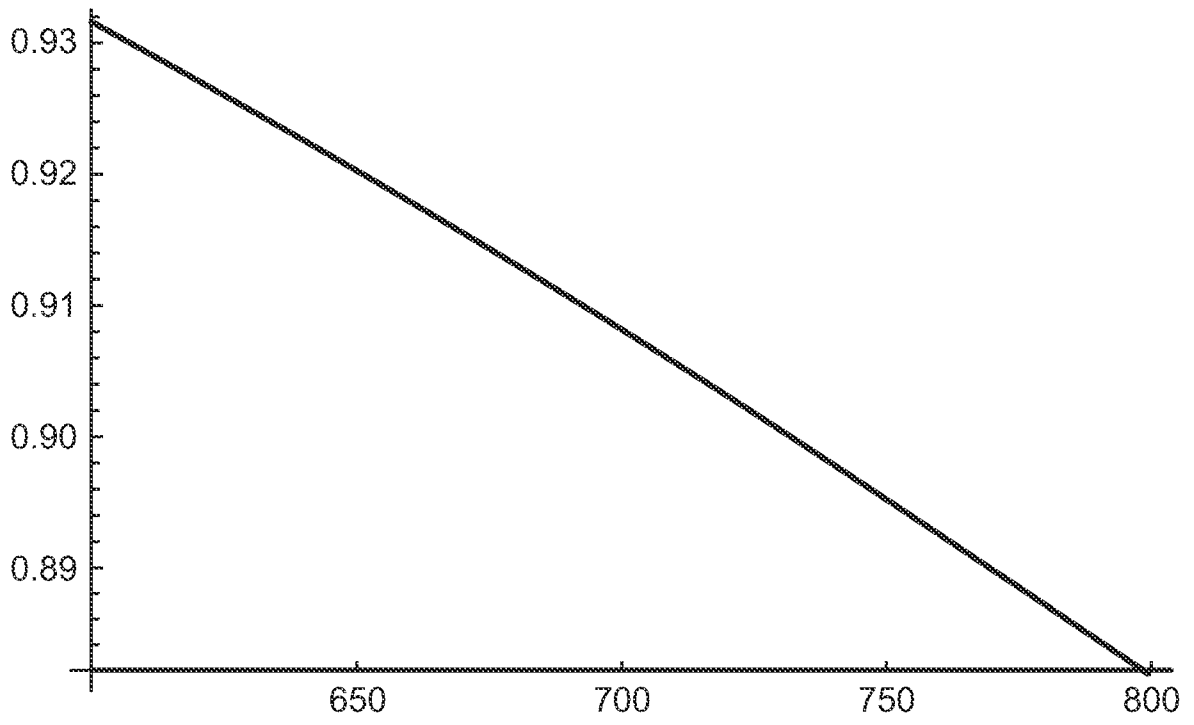


FIG. 12

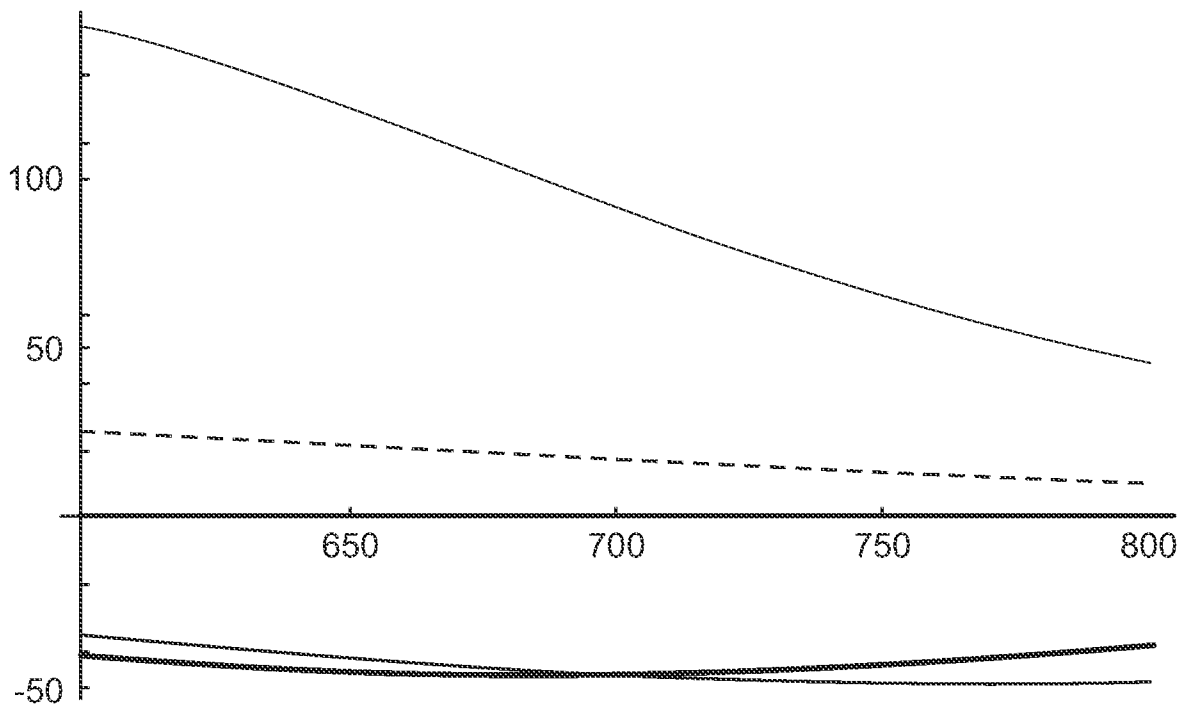


FIG. 13

10/11

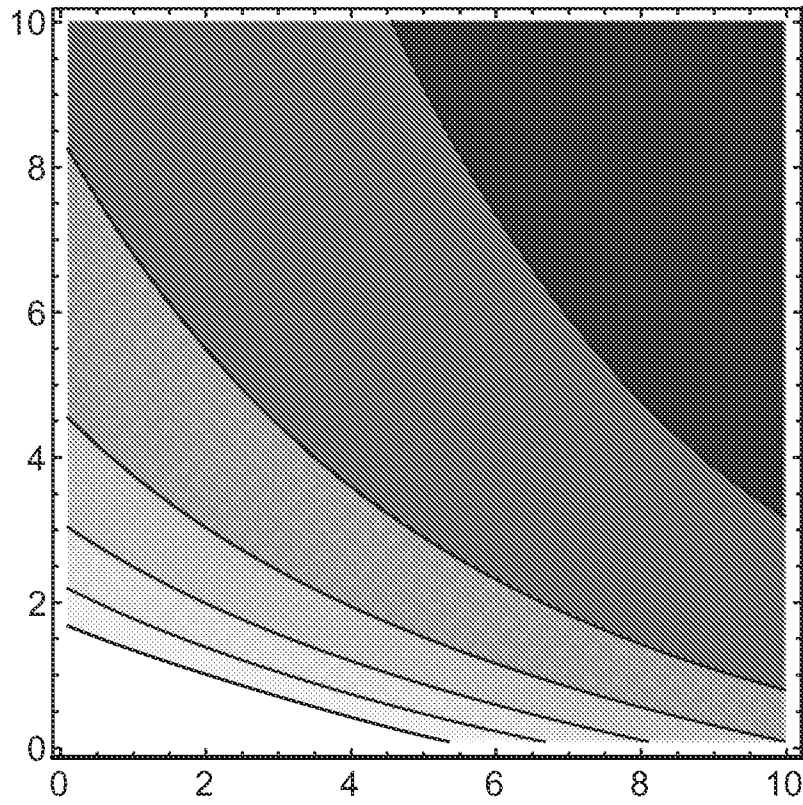


FIG. 14

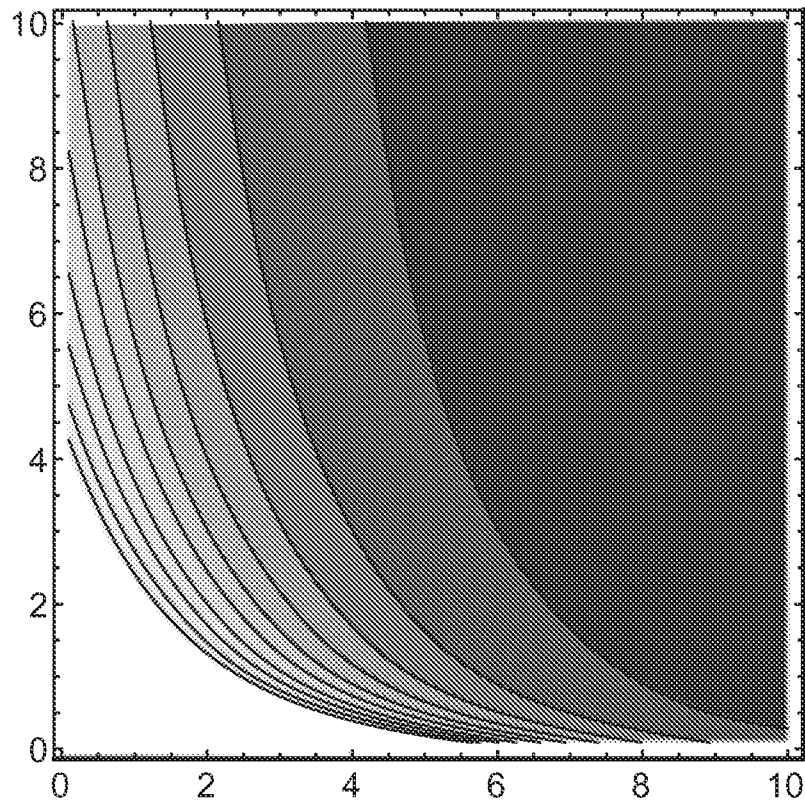


FIG. 15

11/11

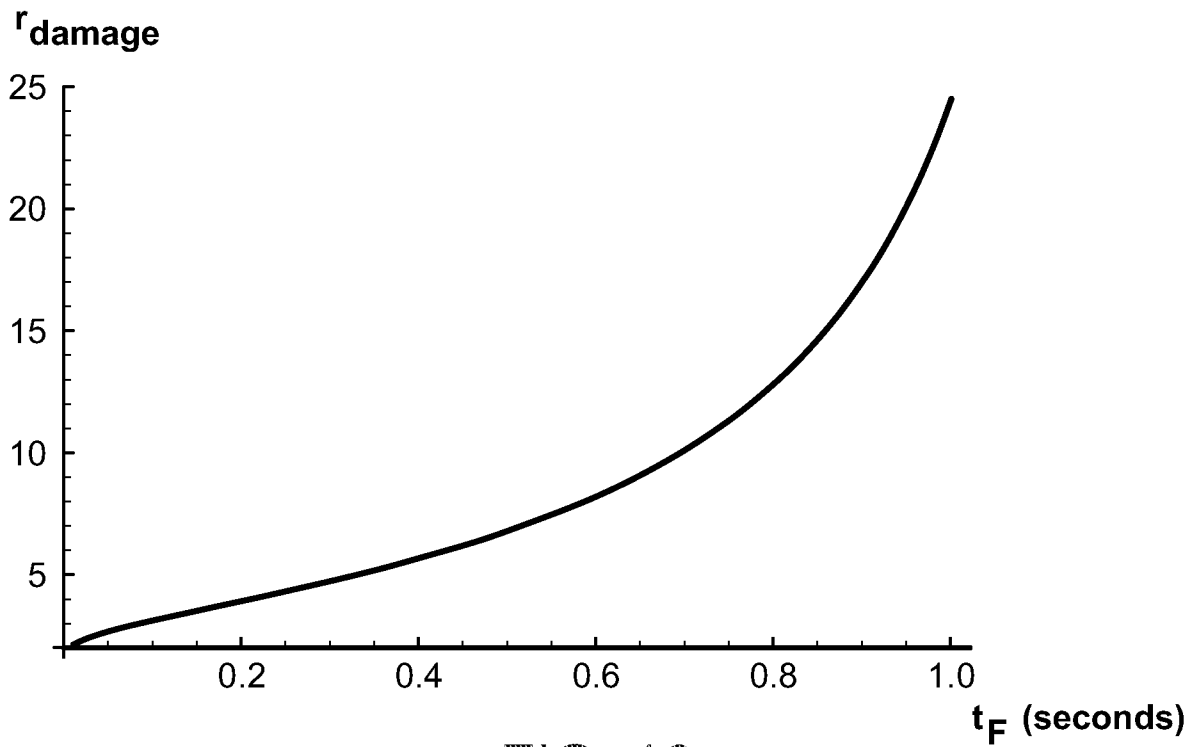


FIG. 16

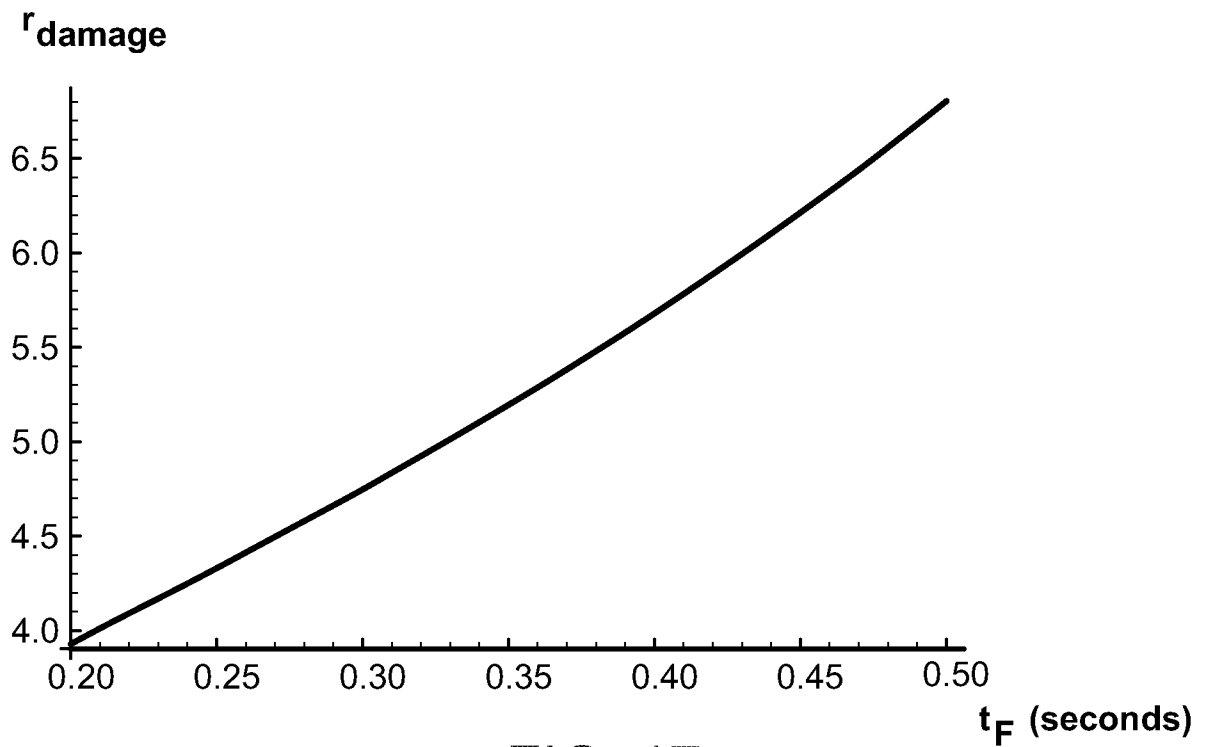


FIG. 17

## INTERNATIONAL SEARCH REPORT

International application No.

PCT/US19/29636

<b>A. CLASSIFICATION OF SUBJECT MATTER</b> IPC - A61F 5/00, 9/00, 9/007, 9/008 (2019.01) CPC - A61F 9/00, 9/008, 9/00802, 9/00821, 9/00823; A61N 5/0613		
According to International Patent Classification (IPC) or to both national classification and IPC		
<b>B. FIELDS SEARCHED</b>		
Minimum documentation searched (classification system followed by classification symbols) See Search History document		
Documentation searched other than minimum documentation to the extent that such documents are included in the fields searched See Search History document		
Electronic data base consulted during the international search (name of data base and, where practicable, search terms used) See Search History document		
<b>C. DOCUMENTS CONSIDERED TO BE RELEVANT</b>		
Category*	Citation of document, with indication, where appropriate, of the relevant passages	Relevant to claim No.
A	US 10,034,796 B2 (TOPCON MEDICAL LASER SYSTEMS, INC.) 31 July 2018; column 2, lines 32-36, column 3, lines 1-15, column 4, lines 25-35, column 7, lines 1-55	1-21
A	US 2012/0029490 A1 (LIN, C et al.) 02 February 2012; abstract, paragraphs [0041] & [0045]	1-21
A	US 2007/0213693 A1 (PLUNKETT, M) 13 September 2007; abstract, paragraph [0050]	1-21
<input type="checkbox"/> Further documents are listed in the continuation of Box C. <input type="checkbox"/> See patent family annex.		
* Special categories of cited documents: "A" document defining the general state of the art which is not considered to be of particular relevance "E" earlier application or patent but published on or after the international filing date "L" document which may throw doubts on priority claim(s) or which is cited to establish the publication date of another citation or other special reason (as specified) "O" document referring to an oral disclosure, use, exhibition or other means "P" document published prior to the international filing date but later than the priority date claimed "T" later document published after the international filing date or priority date and not in conflict with the application but cited to understand the principle or theory underlying the invention "X" document of particular relevance; the claimed invention cannot be considered novel or cannot be considered to involve an inventive step when the document is taken alone "Y" document of particular relevance; the claimed invention cannot be considered to involve an inventive step when the document is combined with one or more other such documents, such combination being obvious to a person skilled in the art "&" document member of the same patent family		
Date of the actual completion of the international search 27 June 2019 (27.06.2019)		Date of mailing of the international search report <b>12 JUL 2019</b>
Name and mailing address of the ISA/ Mail Stop PCT, Attn: ISA/US, Commissioner for Patents P.O. Box 1450, Alexandria, Virginia 22313-1450 Facsimile No. 571-273-8300		Authorized officer Shane Thomas PCT Helpdesk: 571-272-4300 PCT OSP: 571-272-7774